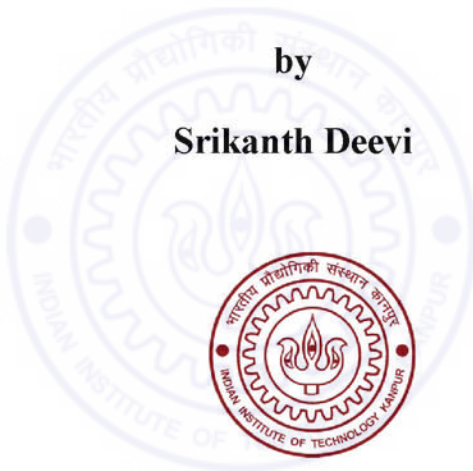


*Seismic Response of Soil Deposits  
With Caissons*

*Thesis Submitted In the Partial Fulfillment of the Requirements for the degree of  
Master of Technology in Geotechnical Engineering*

by

**Srikanth Deevi**



**Project supervisor**

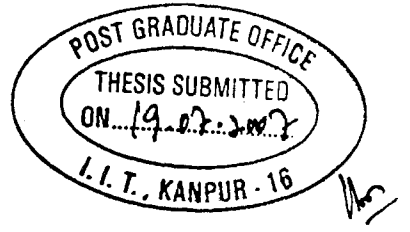
**Dr. Amit Prashant**

**DEPARTMENT OF CIVIL ENGINEERING  
INDIAN INSTITUTE OF TECHNOLOGY KANPUR**

**JULY, 2007**



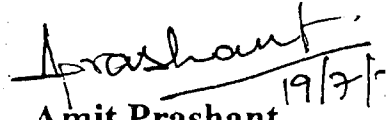
*To My Parents*



## CERTIFICATE

It is certified that the work contained in the thesis entitled "*Seismic Response of Soil Deposits With Embedded Caissons*" by Mr. Srikanth Deevi, has been carried out under my supervision and that this work has not been submitted elsewhere for a degree.



  
Amit Prashant

Assistant Professor

Department of Civil Engineering

Indian Institute of Technology Kanpur

Kanpur-208016, India

19 July, 2007

## **ACKNOWLEDGEMENT**

I take this opportunity to express my sincere gratitude to Prof. Amit Prashant for suggesting the present problem and for his constant involvement, motivation, guidance and encouragement at the various stages of this thesis work. It is only through his valuable suggestions and fatherly care that I could overcome my shortcomings associated with the present work. His patient hearing, critical comments and approach to the present problems have helped me immensely.

I express my indebtedness to my teachers Dr. P.K. Basudhar, Dr. N.R. Patra and Dr. Sarvesh Chandra for their fruitful suggestions and for enlightening me with new concepts of Geotechnical Engineering and also for their help and continuous support during my stay in the institute.

I also owe my sincere thanks to Silvia Mazzoloni, Opensees site moderator , Changho Choi, PhD, PE, On-Lei Annie Kwok, PhD, University of California, Los Angeles for their valuable suggestions during the simulation and development of GUI. I acknowledge the help rendered by my friends Saurabh Tripathi, Mousumi Mukherjee , vivek varshney and Paramita Bhattacharya. In general, thanks to my entire group of friends for constantly encouraging me and providing me the emotional support.

Finally I would like to express my gratitude to my Parents for their encouragement and support at all times. Lastly I thank the Almighty for being always there for me.

**Srikanth Deevi**

# CONTENTS

<b>List of Figures</b>	iv
------------------------	----

<b>List of Tables</b>	vi
-----------------------	----

<b>List of Symbols</b>	vii
------------------------	-----

## CHAPTER 1 Introduction

1.1 General	1
1.2 One-dimensional ground response analysis	2
1.3 Methods of analysis	
1.3.1 Linear analysis	4
1.3.2 Equivalent linear analysis	4
1.3.3 Non linear analysis	4
1.4 Current design practices	5
1.5 Challenges	7
1.6 Literature review	7
1.7 Opensees command language	9
1.7.1 Graphic user Interface (GUI)	10
1.8 Scope of study and organization of thesis	11

## CHAPTER 2 Critical issues on modeling

2.1 Grid spacing and Numerical damping	15
2.2 Time step	16
2.3 Radiation damping	18
2.3.1 Transmitting boundary	21
2.3.2 Verification of Lysmer boundary	23
2.4 Damping	24
2.4.1 Numerical Damping	24
2.4.2 Transient Analysis	26
2.5 Initial conditions	27
2.6 Soil structure interaction effects	28

2.6.1 Theory of contact elements	29
2.6.2 Ill-conditioning of interface elements	30
2.8 Ground motion parameters	30
2.8.1 Response spectrum	30
2.8.2 RMS acceleration	30
2.11 Evaluation of model	31

## **CHAPTER 3 Two dimensional model**

3.1 Free-field model and analysis	35
3.2 Model of Soil-Caisson System	42
3.2.1 Model description	42
3.2.2 Properties of the Interface elements between soil and caisson	42
3.3 Observations from the analysis	44
3.4 Modeling slip and separation	46
3.5 Interference of shear waves	48

## **CHAPTER 4 Zone of influence**

4.1 Determination of the Zone of Influence Using Peak Acceleration	52
4.1.1 Generating Contour Plots for Variation of Peak Accelerations	52
4.1.2 Interpretation from the variation of peak acceleration contour	53
4.2 Determination of the Zone of Influence Using RMS Acceleration	56
4.2.1 The Influence Zone of Embedded Caisson with Contact Elements	56
4.2.2 The Influence Zone of Embedded Caisson with Rigid Contacts	62
4.3 Summary of Observations from Influence Zone Study	64

## **CHAPTER 5 Conclusions and recommendations**

5.1 Summary and Conclusions	65
5.2 Scope of future studies	67

<b>REFERENCES</b>	68	
<b>APPENDIX 1</b>	Interface between Opensees and Gid	70
<b>APPENDIX 2</b>	Modified Opensees source code and algorithm	75
<b>APPENDIX 3</b>	Ground motion parameters of input motion	77



## List of Figures

- Figure 1.1 Typical sketch of caisson for Railway bridge
- Figure 2.1 OpenSees model for evaluation of model parameters
- Figure 2.2 Response for different element sizes
- Figure 2.3 Displacement Response for different time step
- Figure 2.4 Transmitting boundaries in soil-caisson system
- Figure 2.5 Schematic diagram of Zero-length element
- Figure 2.6 Lysmer boundary and coefficients
- Figure 2.7 Model for verification of Lysmer condition
- Figure 2.8 Response at fixed boundary (displacement Vs time)
- Figure 2.9 Response analysis at transmitting boundary
- Figure 2.10 Rayleigh damping (Zerwer et al, 2002)
- Figure 2.11 SHAKE model
- Figure 2.12 Response spectrum at the top node for model evaluation
- Figure 3.1 2D-Pressure dependent free-field model (Elastic)
- Figure 3.2 Response spectrums at different nodes with damping ratios of 5, 10 and 15 %
- Figure 3.3 Amplification at the surface and 10 m below the surface
- Figure 3.4 Response spectrums at top node and input motion
- Figure 3.5 2D- Soil –well- pier system with contact elements at soil-well interface
- Figure 3.6 Dimensions of Caisson and pier
- Figure 3.7 Response spectra at Input motion and top of the caisson
- Figure 3.8 Response spectrum at top node in free-field and soil-caisson system
- Figure 3.9 Response spectrum at top and bottom of the well
- Figure 3.10 Separation at the Soil-caisson interface
- Figure 3.11 Interference of waves
- Figure 3.12 Wave propagation in the soil-caisson system
- Figure 4.1 Influence zone around the caisson
- Figure 4.2 Contour for the relative change in peak horizontal acceleration
- Figure 4.3 Response spectrum at a 4 m away from caisson at top
- Figure 4.4 Response spectrum at a 24 m away from caisson at top

- Figure 4.5 Influence zone for soil-caisson with contact elements along the interface
- Figure 4.6 Variation of RMS acceleration with depth from the ground surface
- Figure 4.7 Percentage variation of RMS acceleration from Free-field to Embedded Caisson condition
- Figure 4.8 Variation of RMS acceleration with distance from the caisson Embedded Caisson with Rigid Contacts with soil List of Tables
- Figure 4.9 Variation of RMS acceleration with distance from the caisson for case: 1



## **List of Tables**

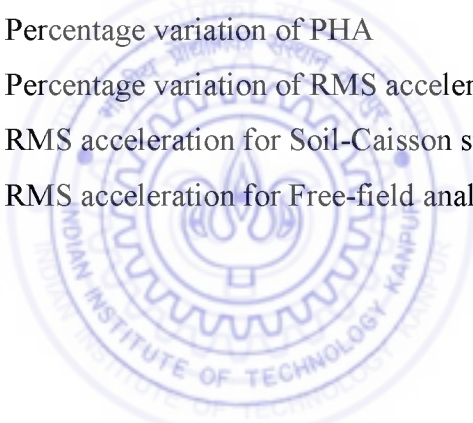
- Table 2.1 Material properties of the 2-D model for evaluation of model parameters  
Table 3.1 Material properties of the 2-D model for the analysis of free-field motion and Soil-Caisson system



## List of Symbols

$\lambda_{\min}$	Minimum Wave length
$f_{\max}$	Maximum frequency
$\Delta h$	Grid spacing
$\Delta t$	Time step
$\xi$	Damping ratio
$\alpha$	Mass proportional damping
$\beta$	Stiffness proportional damping
$V_s$	Shear wave velocity
$V_p$	Primary wave velocity
$C_N$	Dashpot co-efficient normal to the boundary
$C_P$	Dashpot co-efficient parallel to the boundary
[M]	Mass matrix
[C]	Damping matrix
[K]	Stiffness matrix
[D]	Elastic constitutive matrix
$\omega_n$	Natural frequency of $n^{\text{th}}$ mode
$\omega_o$	Predominant circular frequency of loading
$\sigma$	Normal stress
$\tau$	Shear stress
$\gamma$	Shear strain
$\epsilon$	Normal strain
$K_s$	Shear stiffness
$K_N$	Normal stiffness
$T_d$	Duration of strong motion
$a_{\text{rms}}$	RMS acceleration
$\lambda_o$	Average intensity
$E$	Elastic modulus
$G$	Shear modulus
$\nu$	Poissons ratio
$\rho$	Density of the material

$f_{\max}$	Maximum frequency of the input motion
$\ddot{u}$	Acceleration
$u$	Displacement
$\chi$	Constant
$f_N$	Force normal to boundary
$f_P$	Force perpendicular to boundary
$P$	Total vertical load
$M$	Moment
$Z$	Section modulus
$A$	Cross-sectional area
$FOS_{slide}$	Factor of safety against Sliding
$FOS_{over}$	Factor of safety against Overturning
$\zeta_p$	Percentage variation of PHA
$\zeta_r$	Percentage variation of RMS acceleration
$RMS_{SC}$	RMS acceleration for Soil-Caisson system
$RMS_{FF}$	RMS acceleration for Free-field analysis



## ABSTRACT

Caissons are massive rigid deep foundation systems for bridges, offshore structures as deep water anchors. These are hollow thin walled cylindrical structures which have a top cap and bottom plug. Caissons sometimes offer as an alternative to pile group. This research deals with the seismic response of soil near a massive rigid circular well-foundation embedded in a finite soil stratum. A 2-D FEM model of soil and well-structure with a rock layer (homogenous half-space) at the bottom is considered and the dynamic response of the soil due to long rigid inclusion is studied for the kinematically induced loading arising from vertical seismic shear-wave propagation. The soil near embedded structures is often modeled using springs and dashpots and free-field ground acceleration response with depth is used to define the representative loading on such a soil-structure interaction model. Since the shear-waves travel much faster in concrete than soil, the waves transmitted through the concrete structure of well foundation in the upper soil mass may reach before the free-field vibrations. As a result, the displacement/acceleration response of the soil adjacent to the well-foundation may be significantly different from the free-field response. Since a massive well foundation can carry a considerable amount of energy through them, it becomes imperative to study the influence zone of such interaction around the inclusion. The soil is considered as a linear visco-elastic material and the far-field boundary is simulated by Lysmer boundaries. The time domain solution is compared with the frequency domain solution. The critical issues of modeling such as element size, absorbing boundary, time-step size and Rayleigh damping parameters are discussed. The soil-structure interface has been modeled using contact elements considering their effect on the waves transmitted to soil through well-foundation. The main objective is to evaluate the influence zone of soil around caisson considering vertical propagation of earthquake shaking, effect of interference of shear waves, initial stress state, interface effects such as loss of contact of well with soil.

# CHAPTER 1

## INTRODUCTION

---

### 1.1 General

Caissons are massive deep foundations and they constitute a major portion of weight of the structure. Caisson foundations deeply embedded in soft soil have been widely used to support major structures, especially bridges. Monumental examples are the tagus bridge in Portugal, supported on perhaps the tallest (88 m high) caisson in the world; the San-Francisco-Oakland bay bridge whose major pier was supported on a 75 m high caisson. These are also called as well foundations in India. Historic structure like tajmahal was built on caisson foundations. Despite their large dimensions, caissons have been shown not to be immune to seismic loading as it was believed for several years (Gerolymus, 2000). This was confirmed in Kobe (1995) earthquake, which caused many structures founded on caissons to suffer severe damage. The seismic response of caissons has been of considerable interest for many years. A number of methods of varying degrees of accuracy, efficiency and sophistication have been developed.

Caissons have better advantages over pile foundations. Open caissons can be sunk much deeper levels as compared with piles. As the caissons have a large contact area it offers better resistance to lateral loads. Caissons offer better lateral load resistance than pile foundations. As most of the material is on the periphery of the caisson it has a large unsupported length than pile foundations.

Following are the four types of caissons

- 1) Box caissons are prefabricated concrete boxes with base and side walls. These are of various shapes and comprise hollow bodies with water tight floors and walls. These types of caissons are used to support large bridges, under water tunneling in and in harbor constructions (jetties, quay walls etc.).

- 2) Open caissons are open at top and are suitable in soft soils, but not where the ground have more obstructions. While sinking the well the interior portion is kept dry by continuously pumping out water and the friction between the soil and caisson is minimized by filling bentonite slurry around the structure.
- 3) In suction caissons, air pressure is maintained inside the concrete shell to prevent water from entering the caisson. These caissons have the advantage of providing dry working conditions which are better for placing concrete and well suited for foundations for which other methods might cause settlement of adjacent structures.
- 4) Monolith caissons are larger than other types of caissons but are similar to Open caissons. They are often found in quay walls where resistance to impact from ships was required.

## 1.2 One-dimensional Ground Response Analysis

Ground response analyses are used to predict ground surface motions for development of design response spectra, to evaluate dynamics stresses and strains for evaluation of liquefaction hazards, and to determine the earthquake-induced forces leading to instability of earth and earth-retaining structures. During the analysis these take into account several factors say rupture mechanism at source of an earthquake, propagation of stress waves through the crust to the top of bedrock beneath the site of interest. One-dimensional analysis is widely used to predict free-field ground response in geotechnical earthquake engineering practice. This problem is commonly referred to as site-specific response analysis or soil amplification study (ground motions may get even de-amplified). This is generally the beginning point for most of the seismic studies and a solution to this problem allows geotechnical engineer to:

- Calculate site natural period of vibrations
- Assess the ground motion amplification
- To evaluate various parameters primarily response spectra, for design and safety evaluation of structures
- Evaluate the liquefaction potential

Soil conditions and local geological features affecting the ground response are

- Horizontal extent and depth of the soil deposits overlying bedrock
- Slopes of the bedding planes of the soils overlying bedrock
- Changes of soil types horizontally
- Topography of both bedrock and deposited soils and faults crossing the soil deposits
- Presence of stiff structures in the soil

One-dimensional analysis is based on following assumptions:

1. All boundaries are horizontal and extend to infinity in horizontal direction as well.
2. The response of a soil deposit is predominately caused by SH-waves propagating velocity from the underlying bedrock.
3. The ground surface is level.

### 1.3 Methods of Analysis

1. Linear analysis
2. Equivalent linear analysis
3. Nonlinear analysis

#### 1.3.1 Linear Analysis:

This method is the simplest method of ground respond analysis. This approach is limited to the analysis of linear systems where soil deposit consists of one uniform layer with constant soil stiffness throughout or varying stiffness in such a way that it can be expressed by simple mathematical functions. Since the stiffness of an actual nonlinear soil changes over the duration of a large earthquake, such high amplification levels will not develop in the field.



**Figure 1.1. Typical sketch of caisson for railway bridge**

### **1.3.2 Equivalent Linear Analysis:**

Some cases this approach is much more efficient than nonlinear approach, particularly when the input motion can be characterized with acceptable accuracy by a small number of terms in a Fourier series. Disadvantage of this method is that an effective shear strain in an equivalent linear analysis can lead to an oversoftened and overdamped system when the peak shear strain is much larger than the remainder of the shear strains, or undersoftened, undamped system for nearly uniform amplitudes of shear strains.

### **1.3.3 Nonlinear Analysis:**

It requires a reliable stress-strain or constitutive model. In this method input parameters are not so much well established as these are in equivalent linear analysis. Therefore, a substantial field or laboratory testing program may be required for evaluating such parameters. It is very much useful for estimating effective stresses due to the generation and dissipation of excess pressure during and after earthquake shaking whereas equivalent analysis do not have such capabilities. This method is better than equivalent linear method where strain levels are high.

One dimensional ground response analysis has certain limitations and is particularly applicable to horizontally layered soils for free field ground motion analysis. However the assumptions of one dimensional ground response analysis are not acceptable in many situations due to problem geometry and other modeling constraints. Sloping or irregular ground surfaces, presence of very stiff embedded structures such as caissons, walls, tunnels require two or three dimensional approach due to the complexity involved in wave propagation. Techniques for the solution of these types of problems have been done in frequency domain as well as time domain. Two and three dimensional dynamic response and soil structure interaction problems are most commonly solved using dynamic finite element analysis. Each method has its own assumptions and the modeling parameters have to be carefully checked. Response spectrum method (Frequency domain method) does not allow accounting for material non-linearities (ANSYS Theory manual). Due to this limitation, the present analysis have been performed in time domain (TD).

Several issues regarding size of elements, absorbing boundaries as well as representation of damping in the system have been discussed in the present study.

Modeling of soil-well system involves complex issues. Although the caisson has an axi-symmetric geometry, loading at a general inclination produces a full three dimensional state of stress and strain in the caisson and in the soil. Therefore 2-D and 3-D models are required for evaluation of response of these types of structures. But these analyses require high computational resources and time.

## **1.4 Current Design Practices**

Indian Road Congress (IRC) publication recommended the provisions for design of road bridges in India. The seismic design force for the highway bridges in India is to be taken as per IRC: 6 -2000, Section II: Loads and Stresses. While that for the Railways Bridges is specified by the Bridges Rules of Indian Railways (IRS-1985, 1988). Over the years, approach of both these codes has been static in nature. Dynamic analysis is recommended only for the bridges with very large spans. The seismic forces, as prescribed by these codes, depend upon the seismic zone the bridge is located in, type of soil-foundation system (for bridges on well foundation, these values are highest), and the importance of the bridge.

The specified design forces as per these codes do not depend upon dynamic properties like natural periods of the system. Neither is there any emphasis on ductile detailing of components liable to flexural failure. Both of these codes assume zero seismic forces for the components permanently buried under ground .It should be noted that IS:1893 (Part 1)-2002 ,the current Indian standard code for the estimation of seismic forces on buildings ,suggests that for components between ground level and 30m depth ,the forces shall be linearly interpolated.

More recently in the year 2002, IRC: 6 have made modifications to incorporate the design spectrum approach wherein, it takes account of fundamental natural period to calculate the seismic forces.

For seismic analysis, forces in the well foundation are obtained from appropriate combinations of the following loads: (a) dead loads of superstructure, substructure and

foundation, (b) live loads on superstructure, (c) active and passive earth pressures, (d) skin friction, (e) water current pressure, (f) inertia forces (mass of the superstructure, substructure and foundation up to scour level only ) and (g) hydrodynamic forces [IRC :6,2000; IRC:78,2000; IRS:1985,1997] .For strength design of well foundations , Working Stress Method [IRC:21,2000] and Limit State Method [IRS-1997,1999] are prescribed for highway and railway bridges ,respectively. Stability against sliding and overturning failures of well foundation is checked by obtaining the factors of safety as follows [IRC: 78, 2000]:

$$FOS_{slide} = \frac{Sliding\ force}{Resisting\ force} \quad \dots \dots \quad (1.1)$$

$$FOS_{over} = \frac{Overturning\ moment}{Restoring\ moment} \quad \dots \dots \quad (1.2)$$

Safety against bearing capacity failure is checked by calculating the maximum base pressure, under the most critical load combination, as follows:

$$P_{max} = \frac{P}{A} + \frac{M}{Z} \quad \dots \dots \quad (1.3)$$

where P is the total vertical load of the well foundation, and M is the net moment at the bottom of well. Factors of safety against sliding, overturning and bearing capacity failures should be more than 1.25, 1.5 and 2.0, respectively.

## 1.5 Challenges

Current Indian practices of seismic analysis for bridges have been very simplistic in approach. Till recently, IRC : 6 provisions did not account for dynamics of the system, and the seismic forces prescribed were unrealistically low in comparison to international practices. The new provision as per IRC: 6-2000 has overcome some of the issues with estimation of seismic forces; the overall procedure still remains too simplistic. The procedure to check for the safety and stability of the bridge under the seismic excitation is unrealistic. As per the current practices, seismic forces obtained from the IRC: 6 are applied as static load with active and passive earth pressures at well foundation, water current pressures, dead loads and live loads acting simultaneously .For a combination of

these loads, member forces are calculated for safety check .Similarly, stability against sliding and overturning is checked for these forces. This approach is unrealistic because active and passive earth pressures don't apply in the same manner to a system under seismic excitation as they apply to a static system under monotonous loading.

More complex issues should be taken in to account for more realistic estimation of member forces and system behavior. For example, dynamics of soil and its interaction with foundation system is accommodated. Non-linearity of soil and interface should be considered in the analysis.

## 1.6 Literature Review

One of the most comprehensive studies on the seismic response of flexible and rigid caissons was conducted by Saitoh (2001), who extended Tajimi's (1969) approximation to account for caisson flexibility and for soil and interface nonlinearities (separation and gapping of the caisson from the soil). The analysis was performed in frequency domain with Winkler springs.

Japanese code (PWRI, 1998) for design specification of highway bridges developed a one-dimensional spring model with distributed springs through depth of the foundation and assumes the soil to be in full contact with foundation and ignores the inertia of underground foundation. PWRI, 1998 gives the procedure to calculate the stiffness terms for three translational and rotational directions.

Zdravkovic, et al. (1998), (2001) presented an extensive numerical study of the short term pull-out capacity of caissons in soft clay. The influence of diameter, skirt length and soil-structure adhesion on pull-out capacity of caissons are studied by three dimensional Finite element analysis.

Chang, et al. (2000) developed 2-D FEM models in FLAC and SAP 2000. In FLAC, a 2-D visco-elastic constitutive model was used to represent the dynamic behavior of soil and rock. In SAP2000, soil was modeled as 2-D plane strain elements, while caisson and super-structure are modeled as beam elements. Horizontal acceleration time history wa s applied at the bed rock level. The results of this study indicate that effect of superstructure on the response of the caisson is insignificant.

A comprehensive study on the static and dynamic response of embedded rigid foundations having various plan shapes (ranging from rectangular of any aspect ratio to triangular) have been published by Gerolymos and Gazetas (2006). They developed a generalized spring multi-Winkler model for the static and dynamic response of rigid caisson foundations of circular, square, or rectangular plan, embedded in homogeneous elastic utilizing an efficient boundary-element method, and numerous results from the published literature, they developed closed-form semi-analytical expressions and charts for stiffness's and damping of horizontally and rotationally loaded arbitrarily-shaped rigid foundations embedded in homogeneous soil. Incomplete contact between the foundation vertical walls and the surrounding soil were taken into account by springs. The model, referred to as a four-spring Winkler model, uses four types of springs to model the interaction between soil and caisson: lateral translational springs distributed along the length of the caisson relating horizontal displacement at a particular depth to lateral soil resistance (resultant of normal and shear tractions on the caisson periphery); similarly distributed rotational springs relating rotation of the caisson to the moment increment developed by the vertical shear tractions on the caisson periphery; and concentrated translational and rotational springs relating, respectively, resultant horizontal shear force with displacement, and overturning moment with rotation, at the base of the caisson.

Agarwal (2006) developed 1-D (linear and non-linear) spring models and 2-D plane strain models using SAP2000 accounting for spatial variation in earthquake motion and change in properties with intensity of earthquake shaking. Dynamic participation of the super-structure was ignored and the investigation was done in plane-strain conditions. The conclusion of the study was that 1-D model gives 2.5-3.0 times higher member forces when compared to 2-D models. It was shown that the inertia of soil plays an important role in the response of system and 1-D models neglect the effect of inertia.

Lysmer (1969) suggested a generalized method through which an infinite system may be approximated by a finite system with a special viscous boundary condition using springs and dashpots. The dashpot co-efficient was evaluated based on the properties of the medium and the results agree well with theoretical results for an axi-symmetric foundation vibration problem. The accuracy of the finite element method depends on the ratio

obtained by dividing the length of the side of the largest element by the minimum wavelength of elastic waves propagating in the system. The accuracy depends on the distance from the excited zone to the viscous boundary due to imperfect wave absorption and this error decreases with an increasing ratio between this distance and the minimum wavelength.

Zerwer et al. (2002) proposed a method to quantitatively evaluate the mesh limitations and damping effects of a finite element model applied to simulate transient wave propagation. The effects of spatial temporal discritization and damping can be analyzed for a single element and the interdependence between wave velocities, maximum mesh dimension and time increment are discussed. Numerical damping and Rayleigh damping parameters are discussed. The results of the study are that the main factor affecting the accuracy of the wave propagation simulations is the spatial temporal discretization.

Hui, et al. (2005), developed a simplified 3D structural dynamic FEM model using ANSYS software, considering composite pile-group-soil effects. The soil beside composite body was separated into near-field and far-field parts. The structural members including piles were modeled by space beam or shell elements, and raft-base was divided into thick-shell elements and the soil was modeled using mass-spring elements.

Maheshwari, et al. (2005) studied the effect of frequency of excitation and stiffness of soil on dynamic response of end bearing pile foundations using a three dimensional non-linear plasticity model. The soil-structure interaction effects were neglected and the soil was assumed to be in full contact with pile throughout the analysis.

## **1.7 OpenSees Command Language:**

OpenSees-1.74 command language is employed for the 2-D finite element analysis of the problem and the visualization of geometry and deformed shape has been done using a pre- and post-processing software GID-8.02. OpenSees is an open source software framework created at the University of California, Berkeley's Pacific Earthquake Engineering Center under a project funded by National Science Foundation, USA. Its purpose is to develop applications to simulate the performance of structural and geotechnical systems subjected to different loading conditions and earthquakes.

### **1.7.1 Graphic User Interface (GUI)**

The interface between OpenSees and GID is needed so that the huge amount of output from the analysis done by using OpenSees can be obtained in a particular format so that it can be read by the GID. The details of the interface are shown in the appendix I. The interface has been developed in the C++ programming language. The interface was developed in two parts. First part transfers the meshing data, material properties, loading, constraints and boundary conditions to the OpenSees (Appendix II). The code was written in C++ using TCL library files. The second interface transfers the output from the OpenSees to GID in the format readable by GID to visualize the results. Opensees source code was edited to obtain the results in a particular format. The details of the modified code were given in appendix II.

## **1.8 Scope of Study and Organization of Thesis**

The present study deals with the response of soil-caisson system to a horizontal component of earthquake motion applied at the rock bed. Secondary effects like liquefaction, hydrodynamic forces caused due to earthquake motion are not considered. The soil-structure interaction has been taken in to account by using a compression only material at the interface between soil and caisson. Dynamic participation of super structure has been neglected. Two dimensional plain strain analysis was done, assuming that there is no out of plane deformations. As the three-dimensional transient analysis for this particular problem is computationally expensive the present model was restricted to plane strain analysis. The present study emphasizes on various aspects such as effect of time step, size of element, numerical damping and initial stress conditions of the soil.

The present work was divided in to five chapters. The first chapter gives an introduction to caisson foundations, Opensees command language and the literature review. The second chapter describes about the selection of model parameters and critical issues of modeling such as spatial temporal discritizations, transmitting boundary, and initial stress conditions. Evaluation of the model is done with theoretical solution of one-dimensional ground response analysis program SHAKE2000. The third chapter discusses about the transient two-dimensional model considering the soil-structure interaction along soil-caisson interface. The interface was modeled using zero-length elements available in

opensees. Compression only material is used for the interface between the soil and the caisson. The soil was modeled using elastic component of pressure dependent multi yield material. The fourth chapter deals with evaluation of influence zone of the soil around the caisson by comparing with the free-field response. The response spectrum was evaluated at the nodes around the caisson and compared with corresponding node response from free-field analysis. While calculating the percentage variation between both the analysis RMS acceleration was compared as it represents amplitude as well as frequency content as comparing peak values is not realistic which considers only amplitude.



# **CHAPTER 2:**

## **CRITICAL ASPECTS IN TRANSIENT ANALYSIS**

---

The response of the system depends on many model parameters which include soil properties, characteristics of input motion at different depths, radiation damping, boundary conditions, soil-foundation interaction, size of element and the time step of analysis. For studying the effect of these modeling parameters free-field analysis of soil subjected to horizontal displacement time history (Appendix-3) was performed for the model shown in Figure 2.1 with model parameters described from Table 2.1.

**Table 2.1: Material Properties**

<b>Soil Properties</b>	<b>Value</b>
Elastic modulus KN/m <sup>2</sup>	78.3 x 10 <sup>3</sup>
Density ton/m <sup>3</sup>	2.0
Poisons ratio	0.30
Damping %	5
Damping coefficients	
Side	C <sub>N</sub> =239.66 C <sub>P</sub> =415.1
Bottom	C <sub>N</sub> =415.1 C <sub>P</sub> =239.66

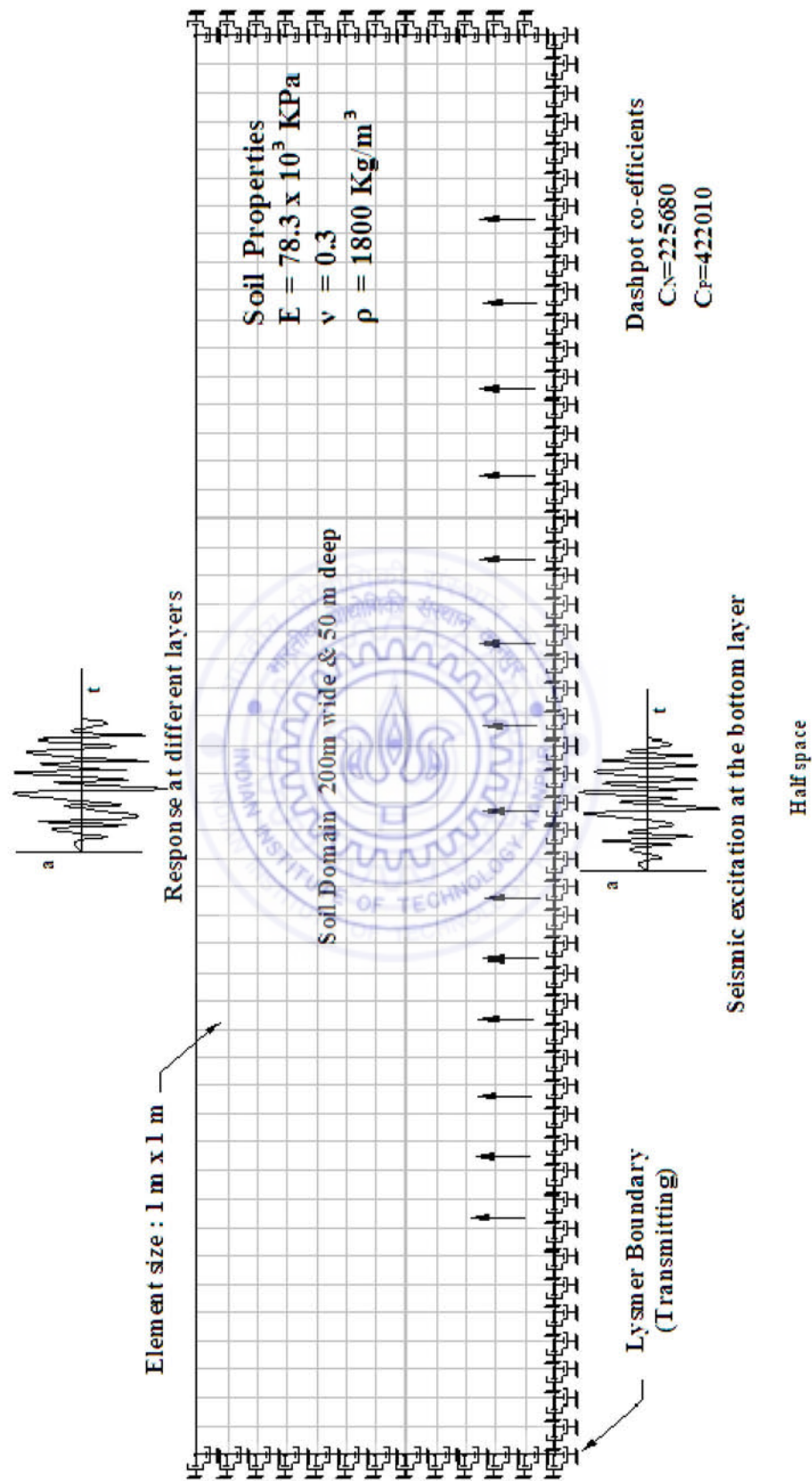


Figure 2.1: OpenSees model

## 2.1 Grid Spacing and Numerical Damping

In the wave propagation problems, the element dimensions are chosen with respect to the highest frequency  $f_{max}$  for the lowest velocity wave  $V_R$ . Element dimensions that are too large will filter high frequencies (Zerwer, 2002) whereas very small element divisions can introduce numerical instability as well as require considerable computational resources.

In order to accurately represent the traveling wave of a given frequency approximately 10 nodes per wavelength are required. Having fewer than 10 nodes per wave length can lead to numerical damping as the discretization misses certain peaks of the wave. In order to determine the appropriate maximum grid spacing the highest relevant frequency  $f_{max}$  that is present in the model needs to be found by performing the Fourier analysis of the input motion. Typically, the value of  $f_{max}$  is about 10 Hz for seismic ground motions.

By choosing a wavelength of  $\lambda_{min} = v / f_{max}$ , where  $v$  is the wave velocity, wavelengths corresponding to a frequency up to 5 times  $f_{max}$  (i.e 50 Hz) can be captured partially. So the smallest velocity is the Rayleigh wave velocity which is 0.9 times of shearwave velocity.

The S-wave and P-Wave velocity of soil can be obtained using the following equations

$$V_S = \sqrt{\frac{G}{\rho}} \quad \dots \dots \quad (2.1a)$$

$$V_P = \sqrt{\frac{G(2-2v)}{\rho(1-2v)}} \quad \dots \dots \quad (2.1b)$$

The maximum grid spacing should not exceed

$$\Delta h = \frac{\lambda}{10} = \frac{0.9 \times V_S}{10 f_{max}} = 1.11m \quad \dots \dots \quad (2.2)$$

where  $V_s$  is the representative shear wave velocity of the soil mass in the simulation. Therefore the element size should not be greater than 1.11 m

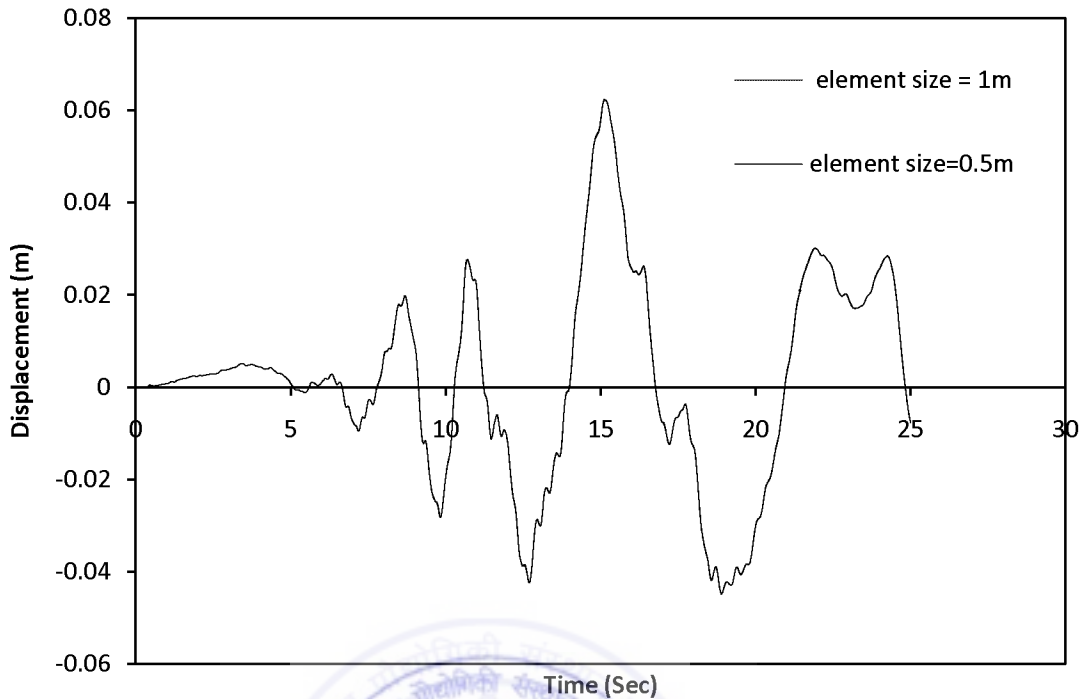


**Figure 2.2: Displacement time history at the top node**

. By using the element size of 1.11 m, the frequency content up to 10 Hz can be captured completely and up to 50 Hz partially. However the response of the system was verified with different element sizes and it was concluded that the reduction in element size below 1 m had no significant effect on the results. The analysis was performed with the element size of 1 m and 0.5 m keeping all the other model parameters constant and the displacement-time history was compared for two cases. Figure 2.1 shows the displacement response at the center top node of the model discretized using square element of the size of 1 m in one case and 0.5 m in the other case. The results for two element sizes overlap exactly indicating no influence of further reduction in the element size below 1 m.

## 2.2 Time Step

The time step  $\Delta t$  used for numerically solving nonlinear vibration or wave propagation problems has to be limited for two reasons. The stability requirement depends on the

numerical procedure in use and is usually formulated in the form of  $\Delta t/T_n$  to be less than a certain tolerance. The parameter  $T_n$  denotes the smallest fundamental period of the system. Similar to the spatial discretization,  $T_n$  needs to be represented by about 10 time steps. While the accuracy requirement provides a measure on which higher modes of vibration are represented with sufficient accuracy, the stability criterion needs to be satisfied for all the modes. If the stability criterion is not satisfied for all the modes of vibration, then the solution may diverge and produce erroneous interpretations. In many cases, it is necessary to provide an upper bound to the frequencies that are present in a system by including frequency dependent damping to the model.

The second stability criterion originates from the nature of the finite element method. As a wave front progresses in space it reaches one point after the other. If the time step in the finite element analysis is too large the wave front can reach two consecutive elements at the same moment. This would violate a fundamental property of wave propagation and can lead to instability. The time step therefore needs to be limited to  $\Delta t < \Delta h/v_s$ , where  $v_s$  is the largest wave velocity and  $\Delta h$  is the element size.

The time increment must be carefully chosen to maintain numerical stability and accuracy. Numerical instability may cause the solution to diverge if the time increment is too large. Conversely a very short time increment can cause spurious oscillations. The calculation of the time increment depends on the element dimensions computed with the following expression given by Zerwer, et al. (2002).

$$\Delta h \leq \chi \lambda_{min} \quad \dots \dots \quad (2.3)$$

$$\text{where } \lambda_{min} = \frac{v_R}{f_{max}}$$

$$\frac{1}{10} \frac{\Delta h}{v_P} \leq \Delta h \leq \frac{\Delta h}{v_P} \quad \dots \dots \quad (2.4)$$

If the size of element is 1m then the time increment should follow  $0.00065 \leq \Delta t \leq 0.0065$ . This implies that the time step should be less than 0.0065 seconds, so all the models in the present study use a time-step of 0.005 sec, as lesser time-step affects the computational resources. The size of the element as well as time step affects the results, if they are not in the prescribed limits mentioned above. Moreover we may not even notice

displacement or acceleration at the nodes if the size of element is larger due to factors mentioned above.

The analysis was performed for the time steps of 0.005 sec and 0.0025 sec and the displacement response has been shown in Figure 2.2. It is evident from this figure that the response was exactly the same for both the time steps. Therefore, a time step of 0.005 sec was followed for all the models in the present study.

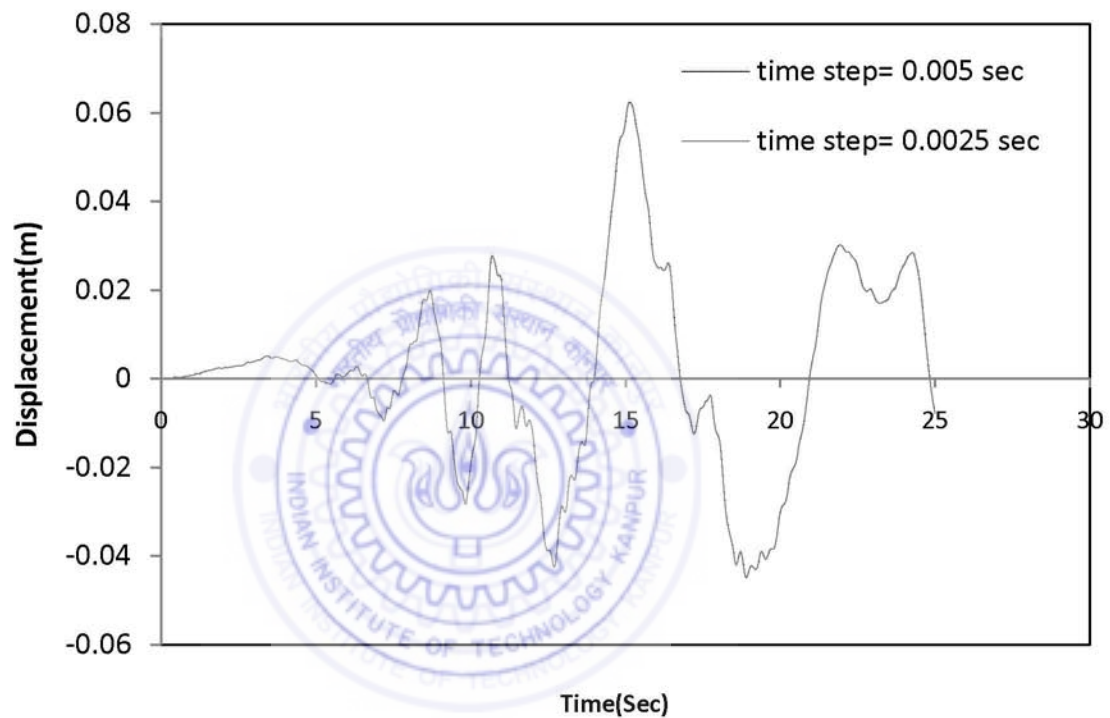


**Figure 2.3: Displacement time history at the top node**

The accuracy and stability of finite element models are primarily affected by the spatial-temporal discretizations within the mesh. In the spatial domain, finite mesh dimensions cause the removal of short-wavelength, (high-frequency) energy. Low pass filtering by the mesh can produce spurious oscillations, known as Gibbs phenomenon, as well as velocity dispersion. To minimize the effects of mesh filtering, the maximum mesh size is calibrated to the wavelength of the slowest propagating wave. Another important factor influencing the numerical accuracy of finite element simulations is the treatment of damping which will be discussed in subsequent sections.

## 2.3 Radiation Damping

One of the biggest problems in dynamic Soil-Structure Interaction (SSI) in infinite media is related to the modeling of domain boundaries. Because of limited computational resources the computational domain needs to be kept small enough so that it can be analyzed within a reasonable amount of time. By limiting the domain however an artificial boundary is introduced. As an accurate representation of the soil-structure system this boundary has to absorb all outgoing waves and reflect no waves back into the computational domain. Early studies (Gomez-Masso, 1978) typically considered seismic analysis assuming that insignificant reflections occur from the lower boundary on which the recorded motion is specified. This is because the wave field consisted mainly of surface waves which do not penetrate deeply into the ground. As the size of the soil domain increases the treatment of boundary conditions becomes significantly important in order to reduce the computational period without compromising the accuracy of interpretations.

Dynamic numerical analysis of geotechnical problems shows decrease in the energy as the domain of interest gets larger. This phenomenon is usually referred to as radiation damping or geometric attenuation, and it is different from material damping in which elastic energy is dissipated by viscous, hysteretic, or other mechanism. The fact that the extent of domain for the analysis in modeling, causes a need for special attention at the boundary. This observation leads directly to the idea of determining the dynamic response of the interior region from a finite model consisting of the interior region subjected to a boundary condition which ensures that all energy arriving at the boundary is absorbed.

To simulate the radiation condition, the “cut off” boundaries must include normal and tangential energy absorption elements. These absorption elements are usually represented by “dashpots”. Using the “dashpots” elements the radiation condition can be easily achieved. The transmitting boundaries at the bottom and sides of the model are shown in Figure 2.3. A schematic of a typical Zero-length element is shown in Figure 2.4. Properly calibrated, these elements absorb the propagating waves in such a way that any incident waves produce zero energy being reflected back into the domain. Even though the energy

absorption depends not only on material properties but also on frequency content, the present study shows that this viscous type of element has enough validity to be used in the practical applications. Although the method is quite simple in concept, its implementation for the analysis of these types of problems presents a formidable computational task. The dashpot coefficients are determined in terms of the material properties of the semi-infinite soil domain.

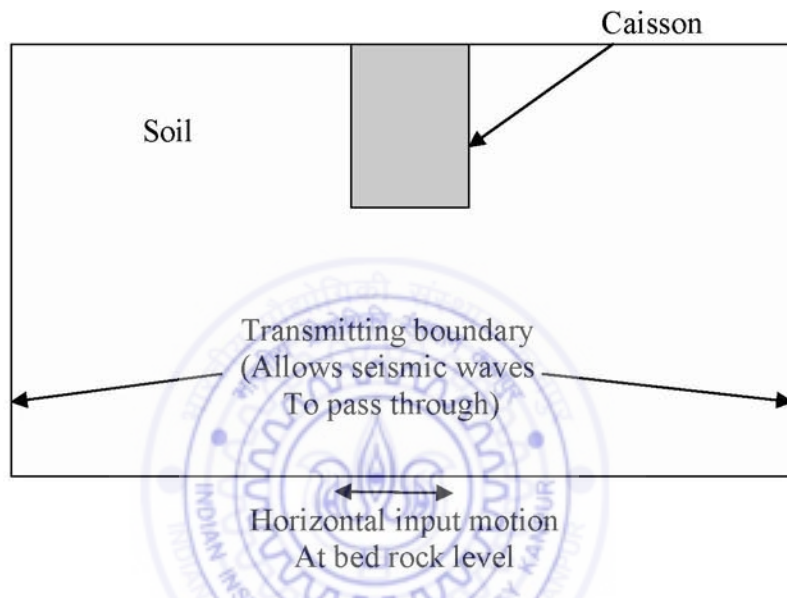


**Figure 2.4:** Transmitting boundaries in soil-caisson system

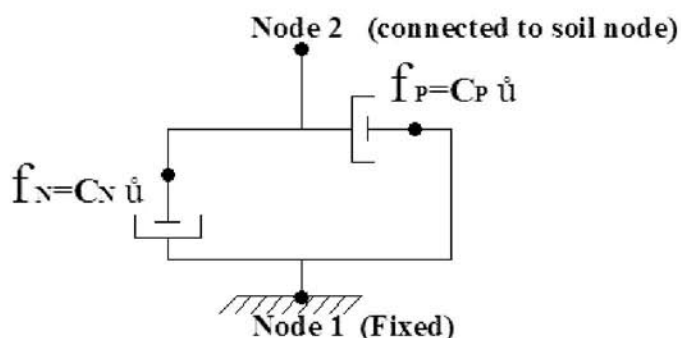


**Figure 2.5:** Schematic diagram of element

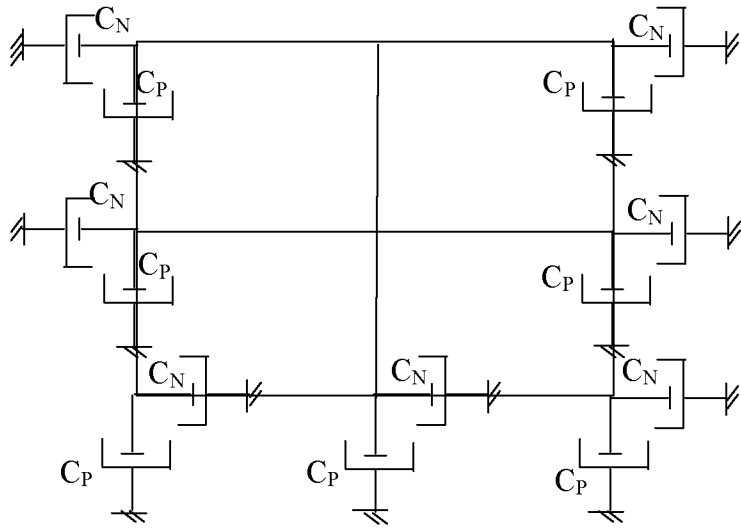


**Figure 2.6: Lysmer boundary and coefficients**

### 2.3.1 Transmitting Boundary

In the finite element model developed during this study, the soil domain was taken as 400 meters in length and 50 meters in depth. Since the soil domain is of finite size, the Lysmer-Kuhlemeyer boundary (Lysmer and Kuhlemeyer, 1969) was used to limit spurious wave reflections at the soil mesh boundary. This boundary could absorb the propagating waves in such a way that the incident wave was transmitted entirely into the soil domain of the finite element model without distortion and no wave was transmitted back to the exterior domain. Since the absorption characteristics of the boundary elements were independent of the frequency, the boundary conditions could be considered perfect absorber of elastic waves for any frequency content of the input motion.

The S-wave and P-Wave velocity of soil can be obtained using the following equations

$$V_S = \sqrt{\frac{G}{\rho}} \quad \dots\dots (2.4a)$$

$$V_P = \sqrt{\frac{G(2-2v)}{\rho(1-2v)}} \quad \dots \dots \quad (2.4b)$$

For the soil properties mentioned in Table 2.1, the above equations give the values of wave velocities as  $V_s = 119.83$  m/sec and  $V_P = 207.51$  m/sec. Using these velocities, the dashpot coefficients for radiation damping can be calculated as given below

$$C_N = \rho * V_s * \text{Element size} = 1.8 * 119.83 * 1 = 239.66$$

$$C_P = \rho * V_P * \text{Element size} = 1.8 * 207.55 * 1 = 415.1$$

The side and bottom boundaries include viscous dashpots in horizontal and vertical directions with coefficients determined from the above steps. The zero-length elements have been used at the boundary for dampers. The zero-length elements have 2 nodes physically at the same location and have a very high stiffness. The preprocessing was done using GID-8.0.2 software. An interface between GID and Opensees using C++ and Tcl scripting language has been developed for preprocessing of the model and post-processing of the results. The details of the Graphical User Interface have been given in the Appendix-2.

The dashpot forces normal ( $C_p$ ) and tangential ( $C_N$ ) to the boundary are determined from the equations given below

$$C_P = \rho V_s \text{ and } C_N = \rho V_P \quad \dots \dots \quad (2.5a)$$

Forces in the dashpot are

$$f_N = C_N \dot{u} \text{ and } f_P = C_P \dot{u} \quad \dots \dots \quad (2.5b)$$

Where  $\rho$  is density of soil,  $v_s$  &  $v_p$  are S-wave velocity and P-wave velocity respectively. On each node at the base and on the lateral boundaries of the soil domain, dashpots normal and tangential to the boundary are provided. The normal dashpots are set to absorb the reflected compressive waves while the tangential ones are set to absorb the reflected shear waves.

In a 3-D or 2-D model the angle of incidence of a wave reaching a boundary can vary from almost  $0^\circ$  to  $180^\circ$ . The Lysmer boundary is able to absorb completely only those

under an angle of incidence of  $90^\circ$ . Even with this type of absorbing boundary a large number of reflected waves may still be present in the domain. By increasing the size of the computational domain the angles of incidence on the boundary can be brought closer to  $90^\circ$  and the amount of energy reflected can be reduced.

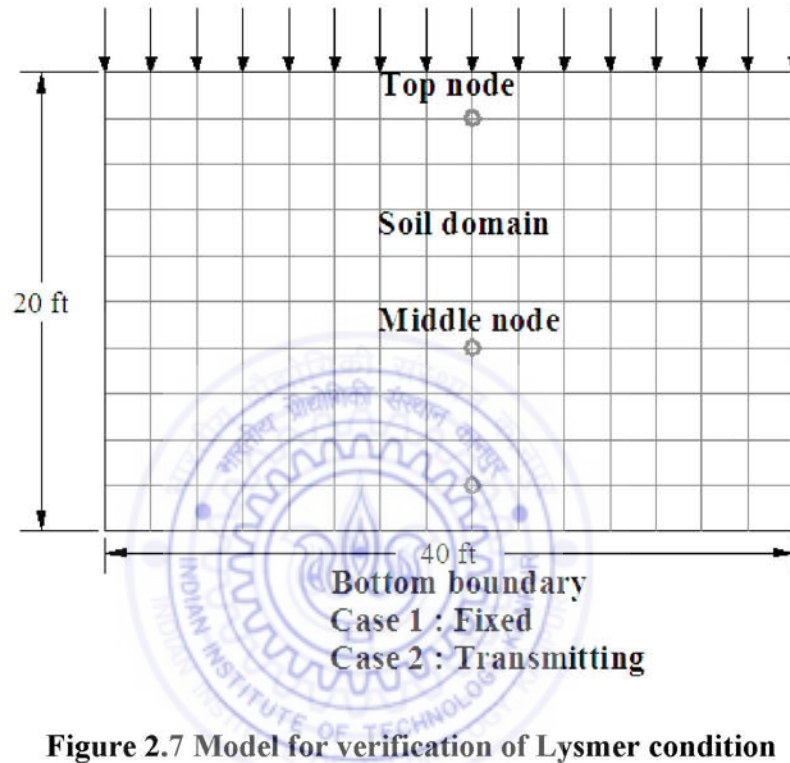


**Figure 2.7 Model for verification of Lysmer condition**

### 2.3.2 Verification of Lysmer Boundary

As verification, a simple 1-D model was analyzed using OpenSees. The 1-D condition was enforced by constraining both the sides of the model to move by the same amount. The analysis was performed using two cases of boundary conditions at the bottom; i.e. "fixed" and "transmitted". Comparison of the recorded displacements at the top and middle nodes showed that the transmitting boundary absorbs most of the incident energy. The distinct reflections observed in the "fixed" case disappear in the "transmitted boundary". A sine and rectangular time series load was applied for a period of 0.4 seconds and the response at different nodes were obtained. The spurious reflections at the fixed boundary can be clearly seen near the node with fixed boundary conditions from

Figure 2.5; whereas, the reflections from the boundary are almost minimum at the same node with transmitting boundary conditions as shown in Figure 2.6. Therefore, the fixed boundary reflected considerable amount of energy which can significantly influence the interpreted response of the structure. The use Lysmer boundary did not prove to be perfectly transmitting boundary and it showed some reflections; however, the magnitude of reflections were considerably lower. These reflected waves can be easily handled by considering a larger width of the model. However, one has to keep in mind that a larger width of the model needs heavy computational resource which further depends on the parameters of analysis.

## 2.4 Damping

Another important factor influencing the numerical accuracy of finite element simulations is the treatment of damping. Two types of attenuation are encountered in the finite element models: numerical and material attenuation. Damping results in energy loss in any dynamic system, which results in decay of amplitude of motion. Although physical damping behavior is quite complicated, the mathematical representation tends to be simplified and is dependent on whether the analysis is transient or mode-superposition methods.

### 2.4.1 Numerical Damping

The Newmark  $\beta$  integration parameters (which control time integration) cause numerical attenuation, whereas Rayleigh damping parameters provide linear material attenuation. Newmark parameters for time integration has been taken as  $\gamma = 0.5$  &  $\beta = 0.25$  (conditionally stable) throughout the analysis as they introduce zero numerical damping. Numerical and material attenuation must be balanced to obtain an accurate model. Hence it becomes quite essential to evaluate mesh limitations and damping effects of a finite element model applied to simulating transient wave propagation. Numerical damping is also caused by the mesh, which removes wavelengths less than Nyquist limit.

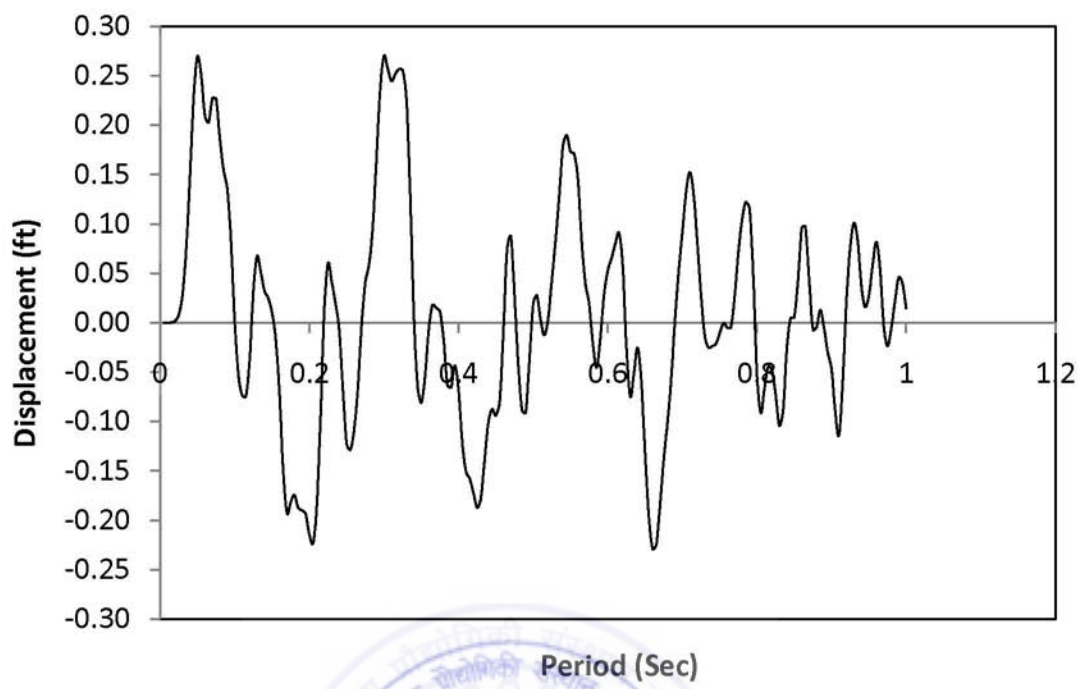


**Figure 2.8: Response with fixed boundary (displacement versus time)**

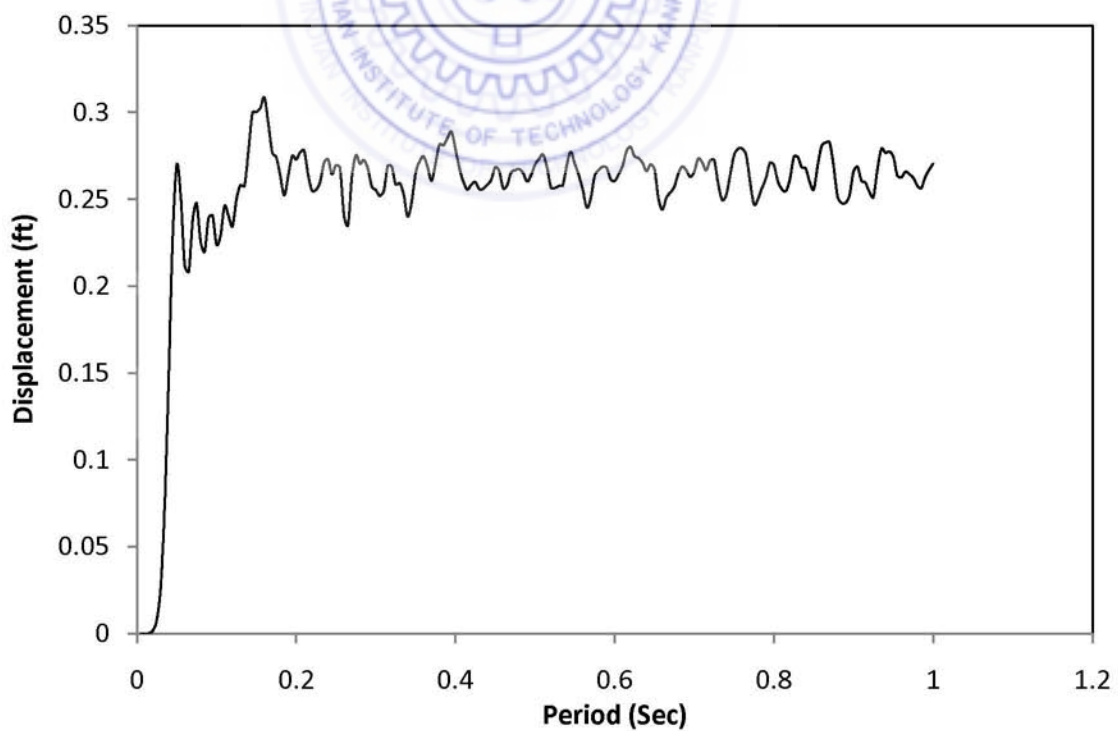


**Figure 2.9: Response with transmitting boundary**

## 2.4.2 Transient Analysis

In dynamic finite element analysis, the governing equation of motion is expressed as

$$[M]\{\ddot{u}\} + [M]\{\dot{u}\} + [K]\{u\} = \{F\} \quad \dots \dots \quad (2.6)$$

Where  $\ddot{u}$ ,  $\dot{u}$  and  $u$  are the acceleration, velocity and displacement vectors, respectively. The mass matrix is given by  $M$ , the viscous damping matrix is  $C$ , and the stiffness matrix is  $K$ . Although energy principles are used to evaluate mass and stiffness matrices, damping matrix ( $C$ ) is not easily incorporated in to finite element solution unless some assumptions are made. Caughey (1960) showed that the damping matrix could be expressed as a linear combination of the mass and stiffness matrices. This type of damping is known as Rayleigh damping and is given by

$$[C] = \alpha [M] + \beta [K] \quad \dots \dots \quad (2.7)$$

where  $\alpha$  and  $\beta$  are constants for mass and stiffness and is termed as mass and stiffness proportional damping parameters. The relationship between damping ratio and Rayleigh damping parameters is given by

$$\xi = \frac{\alpha}{2\omega_1} + \frac{\beta\omega_1}{2} = \frac{\alpha}{2\omega_n} + \frac{\beta\omega_n}{2} \quad \dots \dots \quad (2.8)$$

where  $\omega_1$  &  $\omega_n$  represent the frequency range and  $\xi$  is the damping ratio.

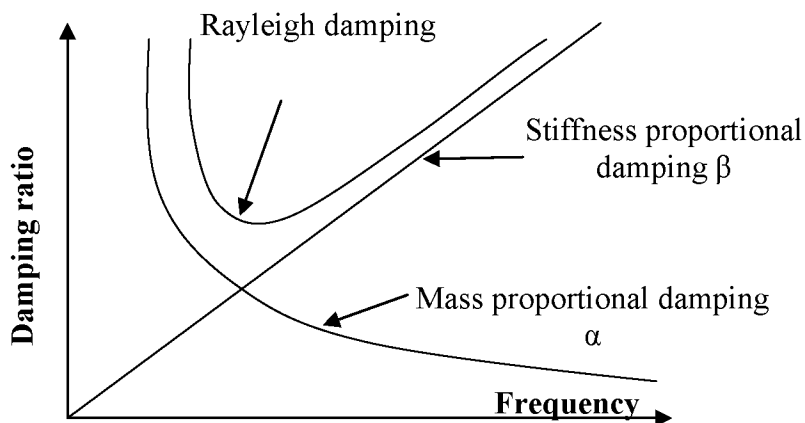


Figure 2.10: Rayleigh damping (Zerwer et al, 2002)

Rayleigh damping parameters were frequency dependent. As discussed in the section 2.4, a constant damping ratio can be defined within a frequency range  $\omega_1$  to  $\omega_n$  using Rayleigh damping parameters. However it becomes difficult to determine meaningful values of  $\alpha$  and  $\beta$  before the start of analysis (Youssef and Duhee, 2002). Beta damping affects higher frequencies and alpha damping affects lower frequencies as shown in figure 2.7. This means that alpha damping should not be used while dealing with large mass method as the large mass would create an artificially high damping force (Sheldon, 1993). Stiffness proportional Rayleigh damping of  $\beta = \eta/G$  has been selected for the present finite element analysis. This choice damps frequencies above 10 Hz appropriately. For conceptual and computational reasons (Gutierrez and Chopra, 1978; Guin and Banerjee, 1998), material damping  $C_m$  is taken as proportional to stiffness and is given by

$$C_m = \beta K \text{ where } \beta = \frac{2\xi}{\omega_0} \quad (2.9)$$

$\omega_0$  = Predominant circular frequency of the loading

$\xi$  = Material damping ratio

$\eta$  = viscosity of material

## 2.5 Initial Conditions

After generation of the Finite element mesh, before the soil well system is analyzed for transient loading, the initial conditions in the ground must be established. This can be achieved by modeling the complete geological history, if it is known. If it is not known the initial conditions can be achieved in two stages.

In the first stage, the conditions appropriate to a Greenfield site are specified as input into the analysis. This can be done by directly specifying the distribution of vertical and horizontal effective stresses in the ground prior to any constructional activity. This can be done by material unit weight, the co-efficient of earth pressure at rest, initial void ratio or by specifying any hardening parameters that is used to model the soil behavior. The second stage involves simulating any previous construction activities that have occurred at the site. However this stage can be eliminated when the previous construction activities have caused minimal disturbance to the in-situ soil conditions.

The ‘Greenfield’ conditions are unmodified initial stresses that exist within the ground, arising from various geological processes that it has been subjected to. These stresses have not been modified by construction. The structure may have to resist these stresses either in whole or part as some stress may be partially relieved before structure is constructed. The geological process that the soil has been subjected to, will determine the ratio of horizontal to vertical effective stress (i.e. the value of  $K_0$ ). This ratio can have an enormous influence on soil behavior and consequently the performance of any structure within it, as demonstrated by Potts and Fourie (1986).

## 2.6 Soil-Structure Interaction Effects

As the seismic waves propagate through soil during an earthquake, a discontinuity in the medium of wave propagation is encountered at the interface of the soil and structural foundations. The change in the material properties leads to scattering, diffraction, reflection and refraction of seismic waves at this soil-foundation interface thereby changing the nature of ground motion at that point from what would have otherwise been observed in free-field response. Further the seismic wave propagates by deformations in the soil medium. As the foundation is considered to be rigid than surrounding soil, the deformation at the soil foundation interface are constrained as the foundation cannot deform by the same amount as surrounding soil. This further leads to slippage across the soil-foundation interface. Moreover, the rigid foundation acts as a low-pass filter by averaging out the high frequency components in the seismic motions. Therefore, the kinematic interaction effects as well as the inertial interaction effects need to be considered during simulations. As the caisson is several times stiffer than the soil, soil-structure interaction effect has significant effect on the response of the whole soil-caisson system when subjected to seismic loading.

The interface properties between the caisson and the soil can have a dominating effect and must be accurately modeled in the analysis. The most appropriate way of doing this is to include interface elements within the mesh. There are several methods to model soil-structure interfaces. Of these, the use of the zero-thickness interface elements is probably most popular. The selection of normal and tangential stiffness of the interface elements is very important as very lower values dominate caisson behavior where as large values

cause numerical ill-conditioning.

### 2.6.1 Basic Theory of Contact Elements

The interface stress consists of a normal and a shear component. The normal stress,  $\sigma$ , and the shear stress,  $\tau$ , are related by the constitutive model to the normal and tangential element ‘strains’,  $\varepsilon$  and  $\gamma$ : The interface element ‘strain’ is defined as the relative displacement of the top and bottom of the interface element:

$$\gamma = \Delta u_1 = u_1^{\text{bot}} - u_1^{\text{top}} \quad \dots \dots \quad (2.10\text{a})$$

$$\gamma = \Delta v_1 = v_1^{\text{bot}} - v_1^{\text{top}} \quad \dots \dots \quad (2.10\text{b})$$

where:

$$u_1 = v \sin \alpha + u \cos \alpha$$

$$v_1 = v \cos \alpha - u \sin \alpha$$

and  $u$  and  $v$  are the global displacements in the  $x_G$  and  $y_G$  directions respectively.

Hence:

$$\gamma = (v^{\text{bot}} - v^{\text{top}}) \sin \alpha + (u^{\text{bot}} - u^{\text{top}}) \cos \alpha \quad \dots \dots \quad (2.11\text{a})$$

$$\varepsilon = (v^{\text{bot}} - v^{\text{top}}) \cos \alpha - (u^{\text{bot}} - u^{\text{top}}) \sin \alpha \quad \dots \dots \quad (2.11\text{b})$$

It is important to note that the element ‘strains’ are not dimensionless, but have the same *dimensions* as the displacements (i.e. length).

The elastic constitutive matrix  $[D]$  takes the form:

$$[D] = \begin{pmatrix} K_s & 0 \\ 0 & K_N \end{pmatrix} \quad \dots \dots \quad (2.12)$$

where  $K_s$  and  $K_N$  are the elastic shear stiffness and the normal stiffness respectively. Noting that these stiffness relate stresses (in units of force/(length)<sup>2</sup>) to strains (in units of length) as in Equation (2.11), implies that they must have the units of force/(length)<sup>3</sup>. They therefore have different units to the Young’s modulus,  $E$ , of the soil or structure adjacent to them (i.e.  $E$  has the same units as stress-force/(length)<sup>2</sup>). As it is difficult to

undertake laboratory tests to determine  $K_n$  and  $K_s$ , selecting appropriate values for analysis is therefore difficult.

### **2.6.2 Ill-conditioning of Interface Elements:**

The Zero-interface element is useful for modeling relative slip and opening and closing on a pre-defined surface. Numerical problems can however occur through ill-conditioning of the stiffness matrix and high stress gradients in the interface. If the element stiffness matrices vary in magnitude by a significant amount ill-conditioning occurs. In many situations stress gradients are likely to be high and are increased with increased interface stiffness. Newton-cotes integration tends to improve the numerical behavior of interface elements. Newton-cotes integrator has been used in the present analysis.

## **2.8 Ground Motion Parameters**

Earthquakes produce complicated loading with components of motion that span a broad range of frequencies. The frequency content describes how the amplitude of a ground motion is distributed among different frequencies. Since the frequency content of an earthquake motion will strongly influence the effects of that motion, characterization of motion cannot be complete without consideration of frequency content. Strong ground motions can be quite complicated, and their complete description involves a large amount of data. For engineering purposes, the essential characteristics of a strong ground motion can be described in much more compact form using ground motion parameters.

### **2.8.1 The Response Spectrum**

The response spectrum describe the maximum response of a single degree of freedom (SDOF) system to a particular input motion as a function of natural frequency and damping ratio of the SDOF system. Response spectrum reflects strong ground motion characteristics indirectly, since they are filtered by the response of a SDOF structure.

### 2.8.2 The RMS Acceleration

The response spectrum relates primarily amplitude, frequency content or duration of a ground motion. Since all these parameters are important, ground motion parameters that reflects more than one are very useful. A single parameter that includes the effects of amplitude and frequency content of a strong motion record is the RMS acceleration, which is defined as

$$a_{rms} = \sqrt{\frac{1}{T_D} \int_0^{T_d} [a(t)]^2 dt} \quad \dots \dots \quad (2.13)$$

where  $T_d$  is the duration of the strong motion and  $\lambda_0$  is the average intensity (or mean squared acceleration). Since the integral in equation 2.13 is not strongly influenced by large, high-frequency accelerations (which occur only for a short period) and it is certainly influenced by the duration of motion, the RMS acceleration can be very useful for engineering interpretations.

## 2.9 Evaluation of Model

The present model was done using opensees, a software framework for developing applications to simulate the performance of structural and geotechnical systems subjected to earthquake loadings.

The soil mass was modeled using 4-noded plane-strain quadrilateral elements, which uses bilinear iso-parametric formulation. The plane strain idealization was used for simplifying a 3-D problem to 2-D problem. The idealization works under the assumption that there is no deformation out of plane. The infinite boundaries at bottom and sides were simulated using radiation dampers (Lysmer boundaries). Absorbing boundary was implemented by using uni-axial zero-length elements in vertical and horizontal directions at each node of the vertical and horizontal boundaries. The length of the domain considered is 400 m so as to minimize the affect of reflections in to the domain. Seismic

excitation was applied at the bottom of the soil layer and the displacement response of the model was computed at different nodes.

The uniform mesh was designed by first calculating the maximum mesh dimensions. As discussed earlier, the maximum dimension depended on the Rayleigh wave velocity, the highest propagating frequency, and the proportionality constant  $\chi$ , as shown in equation 2.2. The modeling of soil domain involves complex issues as the boundary has significant effect on the results. Hence, the width of the model should be considerably large so as to limit these reflections in to the domain under interest. The earthquake excitation was applied at the base of the model.

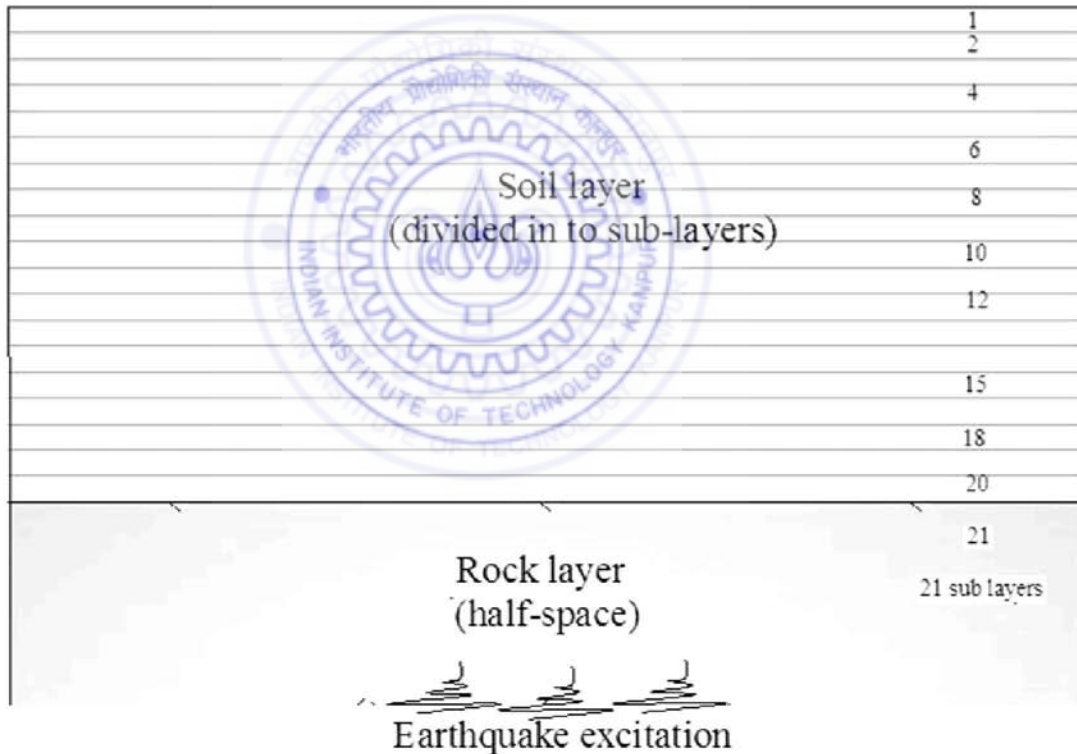
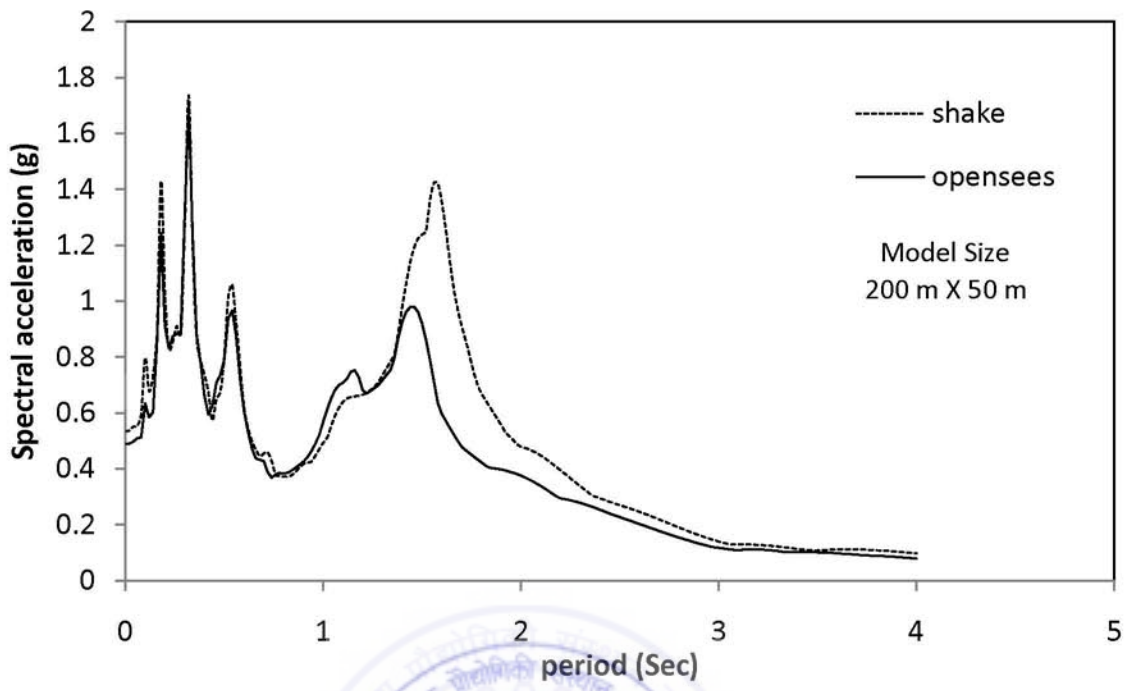
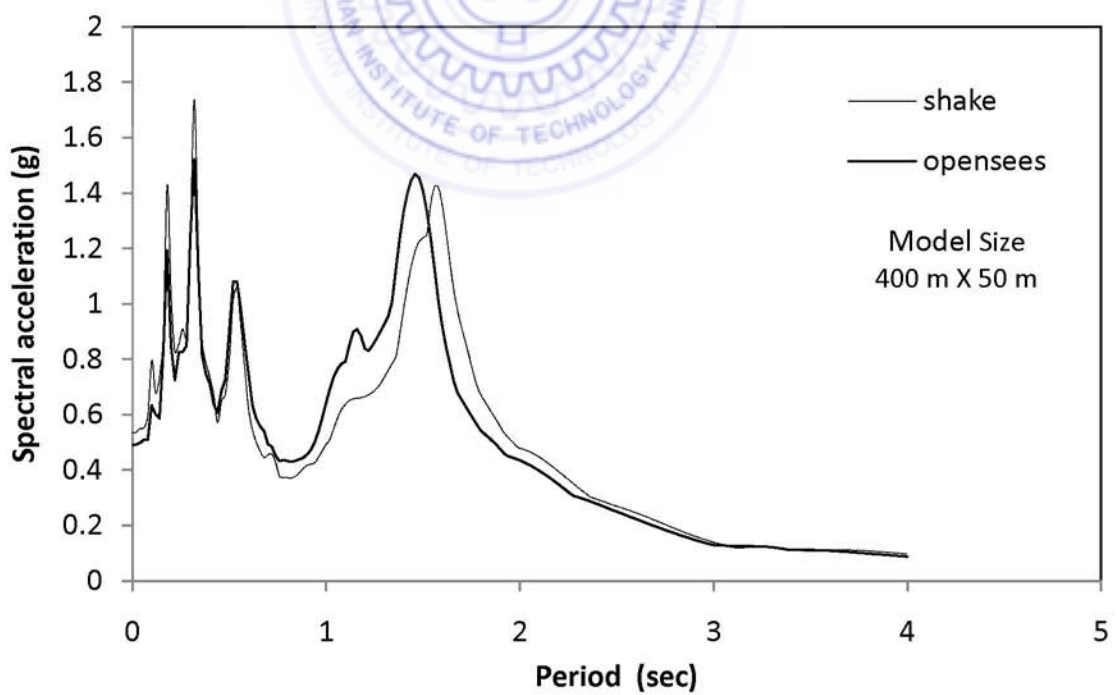


**Figure 2.11: SHAKE2000 model**

The present 2-D model was evaluated with 1-D program SHAKE2000 for free-field ground motions. The soil was assumed to be linear elastic in both the cases. SHAKE2000 required the damping to be defined as frequency independent damping ratio and the analysis was performed in frequency domain. The Opensees framework required Rayleigh damping parameters  $\alpha$  and  $\beta$  which were determined using equation 2.9. From these observations a mesh size of 1m with a time step of 0.005 seconds was followed throughout the study. The stiffness proportional damping was calculated using equation 2.9. The Lysmer transmitting boundary along the side and bottom of the boundary was used throughout the model and the damping coefficients for the zero-length elements were calculated using equations 2.5 (a) and (b). The response spectrum obtained from both the analysis is almost coinciding for both the free-field analysis models as shown in figure 2.10. The frequency domain solution uses a frequency independent damping where as the transient analysis performed using Opensees framework has frequency dependent damping parameters. A constant damping ratio cannot be accurately determined between a range of frequencies. Due to this approximation of damping ratio there is some variation between one dimensional ground response analysis and transient finite element analysis.



(a)



(b)

**Figure 2.12: Response spectrum at the top node**

# CHAPTER 3

## TRANSIENT ANALYSIS OF EMBEDDED CAISSON

---

### 3.1 Free-Field Model and Analysis

A two dimensional finite element model for free-field analysis has been shown in Figure 3.1. The model was analyzed for the horizontal input motion as specified in Appendix 3. The input parameters as size of element, time step, transmitting boundary, interface elements were selected by considering the concerning issues discussed in chapter 2. The free-field analysis was performed on the soil domain to a horizontal seismic excitation at the bottom nodes. The lateral and base boundary conditions for the computational soil domain were modeled using a modified Lysmer transmitting/absorbing boundary. A series of viscous dampers normal and tangential to the soil boundaries were used to implement these transmitting boundaries. The properties of the soil and boundary have been described in Table 3.1.

The soil domain was modeled using four-node quadrilateral plain strain elements based on bilinear iso-parametric formulation. The bed rock was assumed to exist at 50 meters below the ground surface. The size of elements was taken as 1 m in horizontal and vertical directions. The boundary was modeled using zero-length uni-axial material with dampers in both horizontal and vertical directions. The damping coefficients were calculated based on the size of the neighboring quadrilateral elements and the soil properties. An input earthquake displacement time history was applied at the bottom in horizontal direction and the transient analysis was performed for 4000 time steps in order to compute the displacement/acceleration response at different points in the domain.

**Table 3.1 Soil properties for the 2-D pressure dependent (Elastic model)**

<b>Soil properties</b>	<b>Values</b>
Reference confining pressure	80 KPa
Reference Shear modulus	27615 KPa
Reference Bulk modulus	59833 KPa
Pressure dependent co-effecient	0.5
Poissons ratio	0.3
Damping ratio %	5
<b>Concrete properties</b>	
Elastic modulus	23000000 KPa
Poissons ratio	0.15
Damping ratio %	1.5
<b>Interface elements</b>	
Stiffness (Compression only)	23000000 KPa
<b>Damping coefficients</b>	
Side	$C_N = 239.66$ $C_P = 415.1$
Bottom	$C_N = 415.1$ $C_P = 239.66$

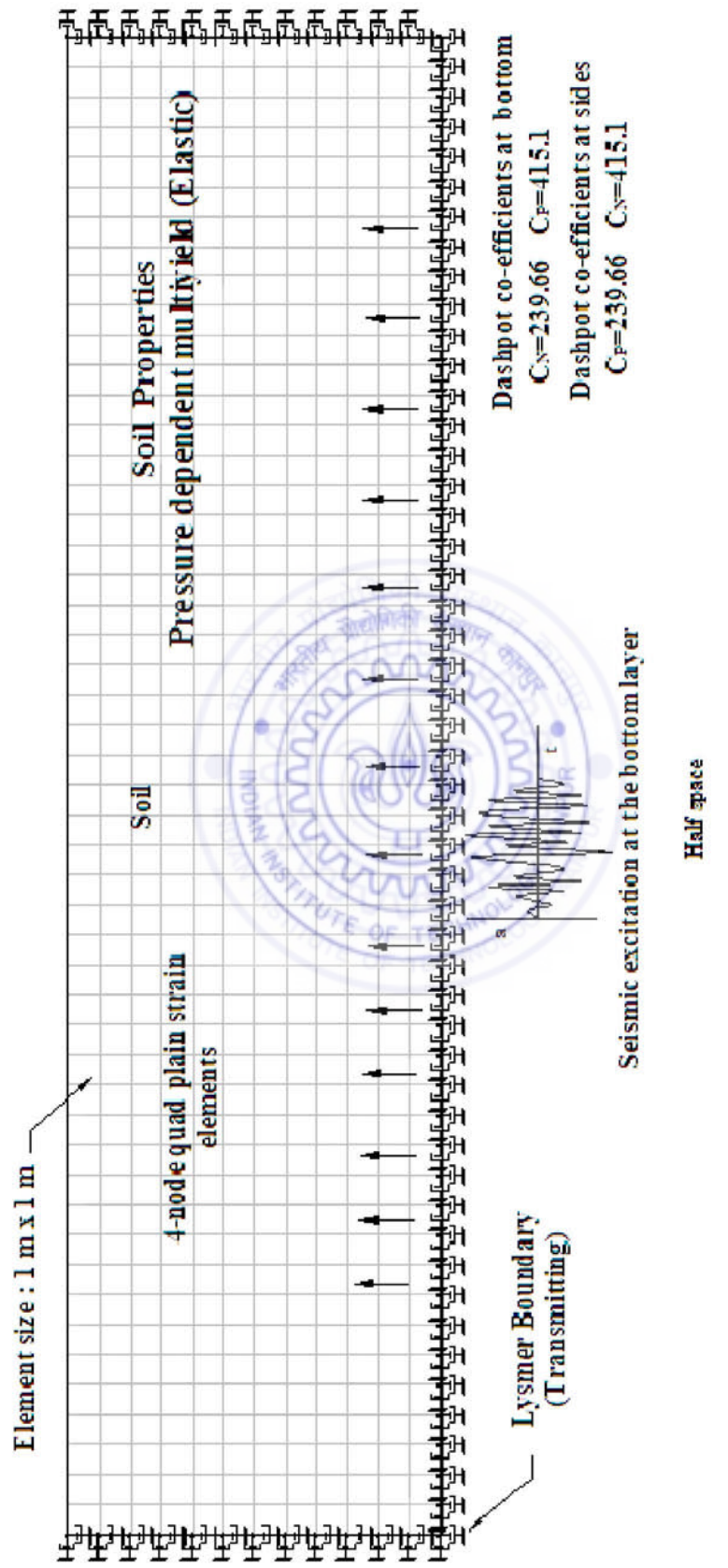
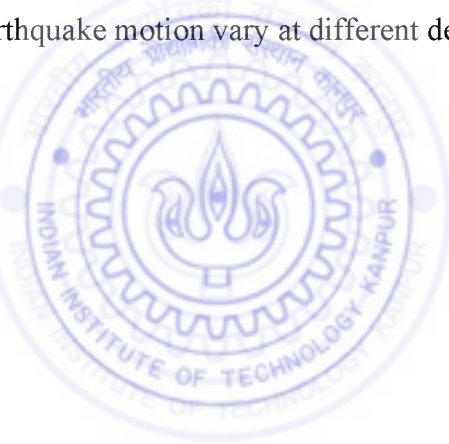
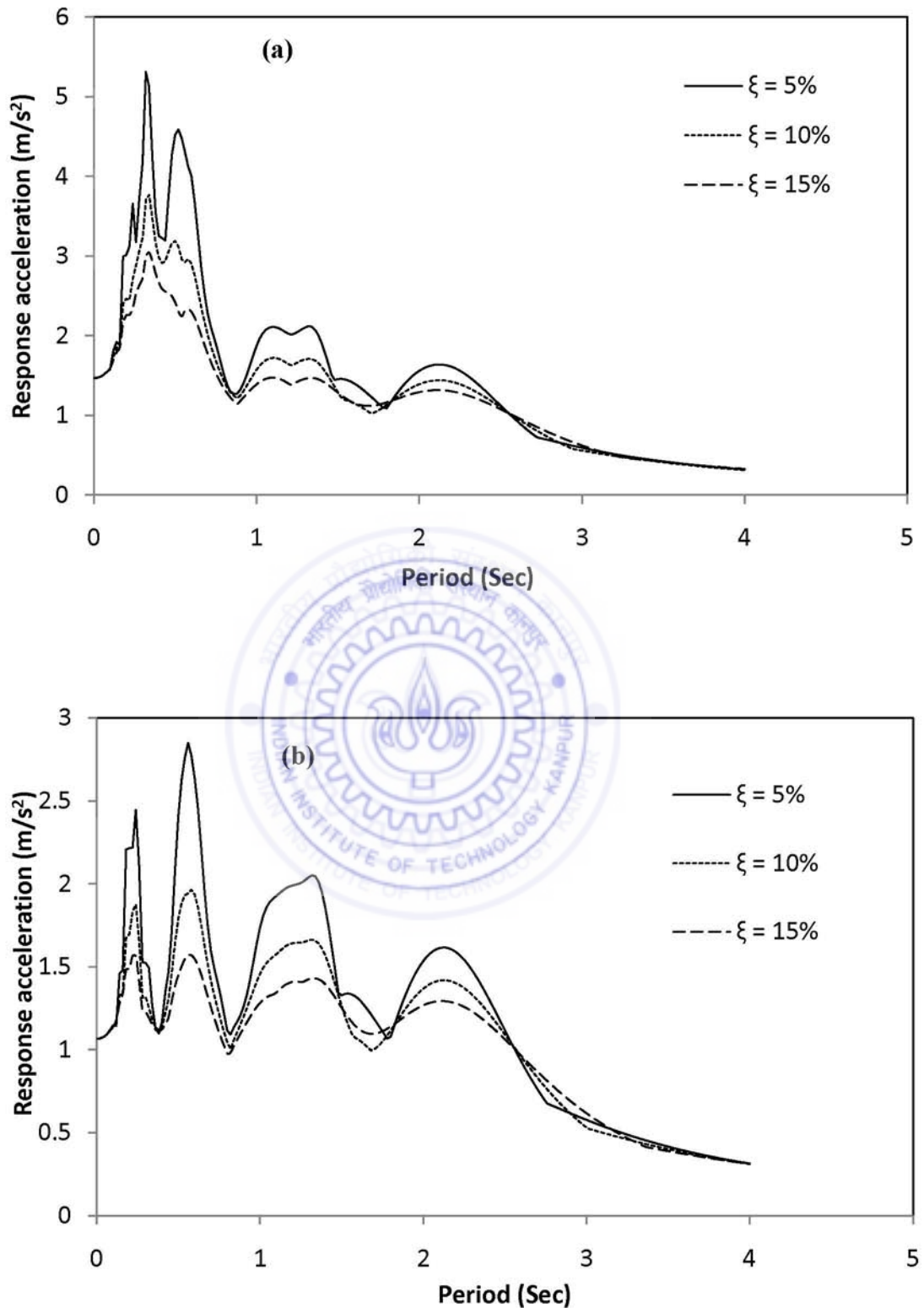


Figure 3.1: 2D-Pressure dependent free-field model (Elastic)

Figure 3.2 shows the response of free-field analysis with varying damping ratios of 5,10,15 % at different depths from the surface of the soil-caisson model. As damping affects the results significantly analysis was performed with different damping ratios in soil domain. The frequencies below 10 Hz are damped with the increase in damping ratio of the soil. The results of the free-field analysis will be used in the subsequent part of the analysis during the study of influence zone around the caisson. Figure 3.3 shows the variation in the response spectrum at the surface and 10 m below the surface. This shows that there would be variation of earthquake motion with depth. Figure 3.4 shows that the amplification of high frequencies begins at the bottom itself and it increases to the top under soil-structure interaction. The presence of well is affecting the frequencies below 10 Hz. The inclusion of the stiff caisson affects the response of the soil-caisson system because the velocity of the wave is much higher in concrete than soil. Intensity and frequency content of earthquake motion vary at different depths below the ground level.





**Figure 3.2: Response spectrum at different nodes with different damping  
at (a) ground Suface (b) 40 m depth (c) 30m depth (d) 20 m depth**

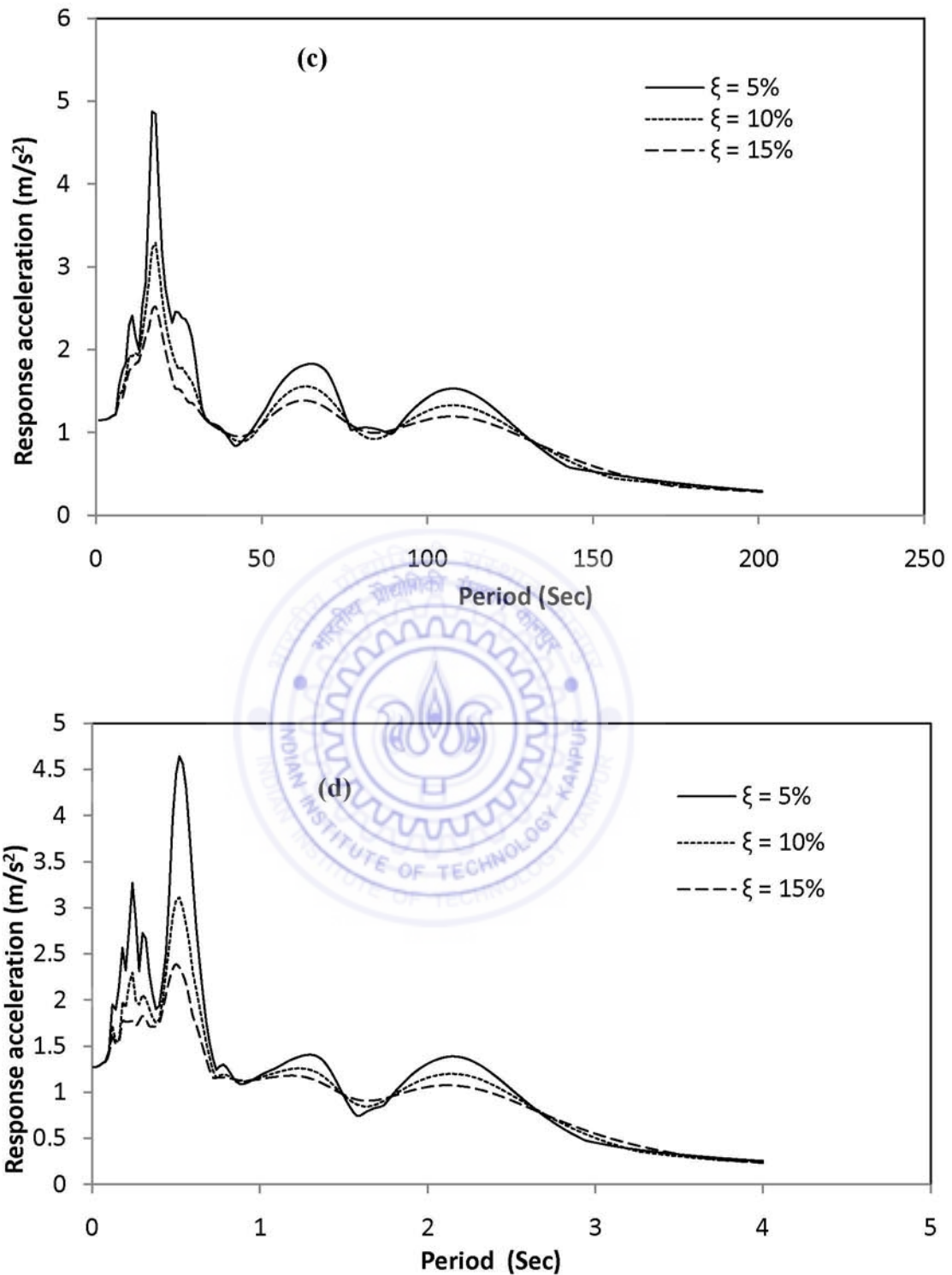
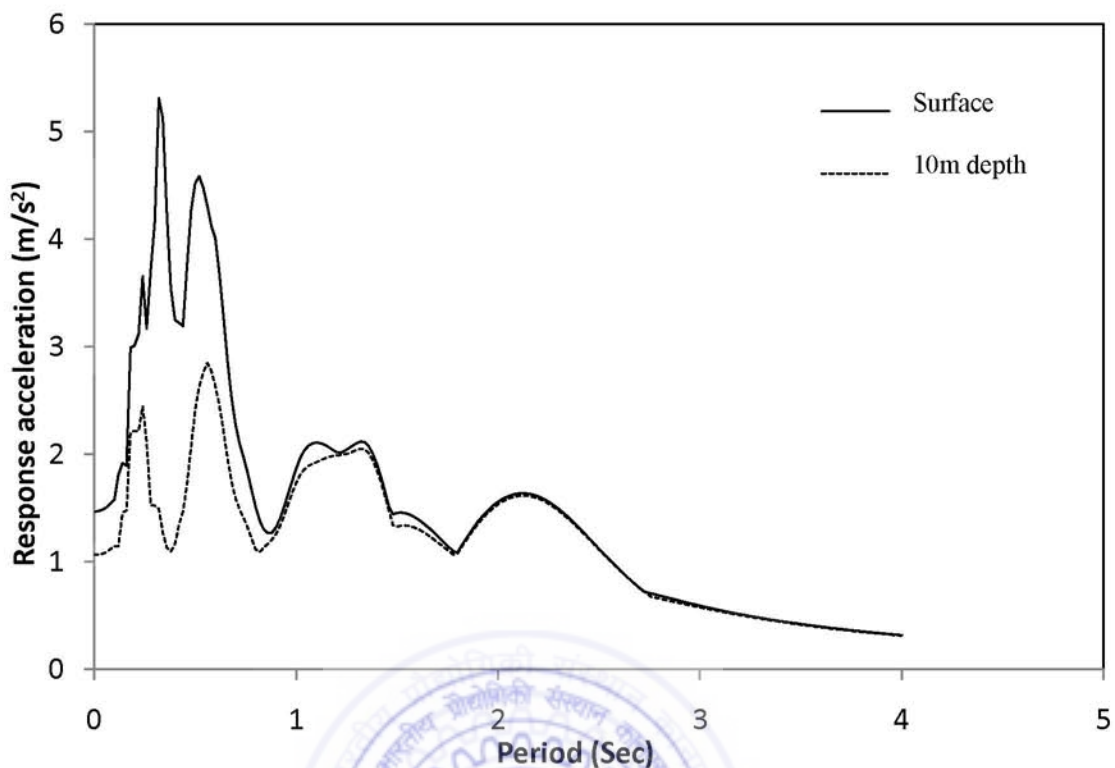
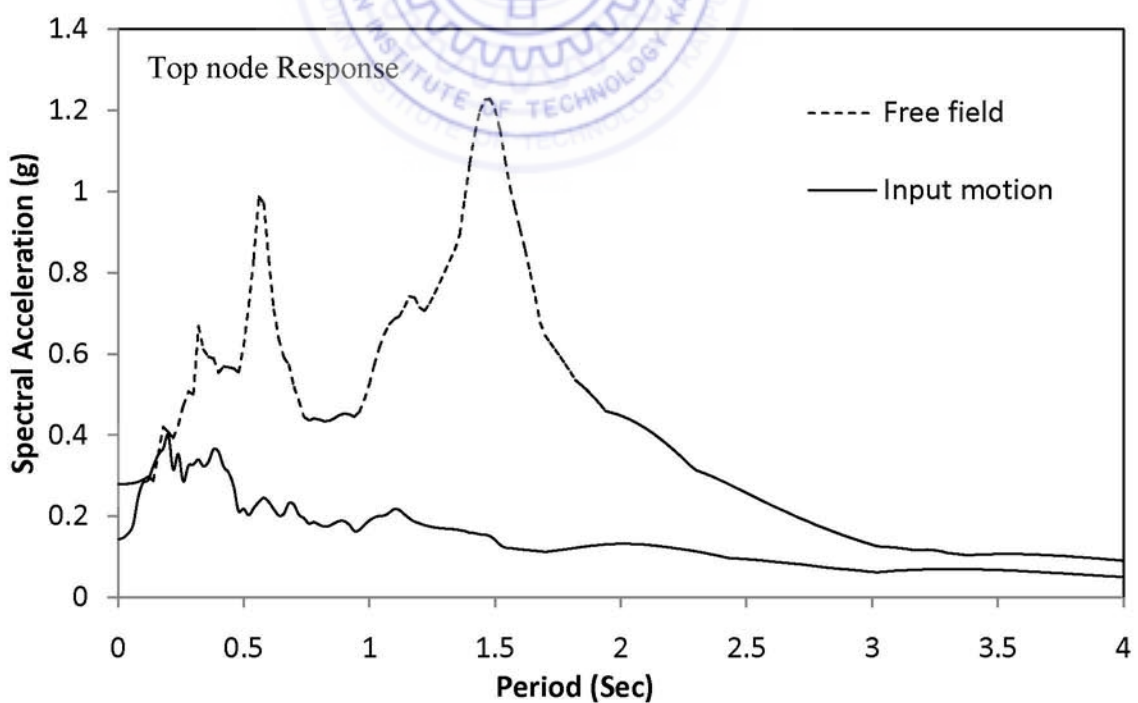


Figure 3.2: Continued



**Figure 3.3: Amplification at surface and 10 m below surface**



**Figure 3.4: Response spectrum at top node and input motion**

## **3.2 Model of Soil-Caisson System**

### **3.2.1 Model description**

The model parameters and boundary conditions for the model of soil-caisson system were similar to the model used for free-field analysis. Figure 3.5 shows the model soil-caisson system. The dimensions of the caisson are shown in Figure 3.6. The properties of the soil and caisson material have been listed in Table 3.1. The width of the model was taken as 400m. The size of the element, damping coefficients and other model parameters were determined based on the previous discussions in Chapter 2.

The rectangular cross-sections of well foundation and pier were modeled using four-node plane-strain and bilinear iso-parametric quadrilateral elements. Square elements of 1m size were used to model soil and caisson. This model accounted for loss of contact around the caisson depending upon the intensity of shaking. Separation and slippage could occur at the soil well interface depending upon the intensity of earthquake shaking as well the other parameters such as stiffness of the contact surface. The response of the system was obtained for the input motion for 4000 time steps.

### **3.2.2 Properties of the Interface elements between soil and caisson**

The soil-caisson interface needs special attention as the wave propagation changes at the interface of two dissimilar materials. In the current study, the contact elements were defined using zero-length elements in Opensees framework. The zero-length elements had two nodes exactly at the same location. One of the nodes was connected to the soil domain and the other to the caisson. The contact element comprised of springs in both X and Y directions with an elastic modulus of concrete in compression  $23 \times 10^6$  KN/m<sup>2</sup>. The material was defined as a compression only material i.e. the stiffness in tension was zero. The stiffness of the contact surface elements can affect the system response significantly because the transfer of stresses between the surfaces in contact largely depends on the contact stiffness. In compressive stress conditions, the stresses can be transferred completely through the contact if the contact stiffness is more than the weaker material. In case of tensile stress, the material will show separation due to the stiffness being zero in tension. Figure 3.9 shows the separation along the soil caisson interface.

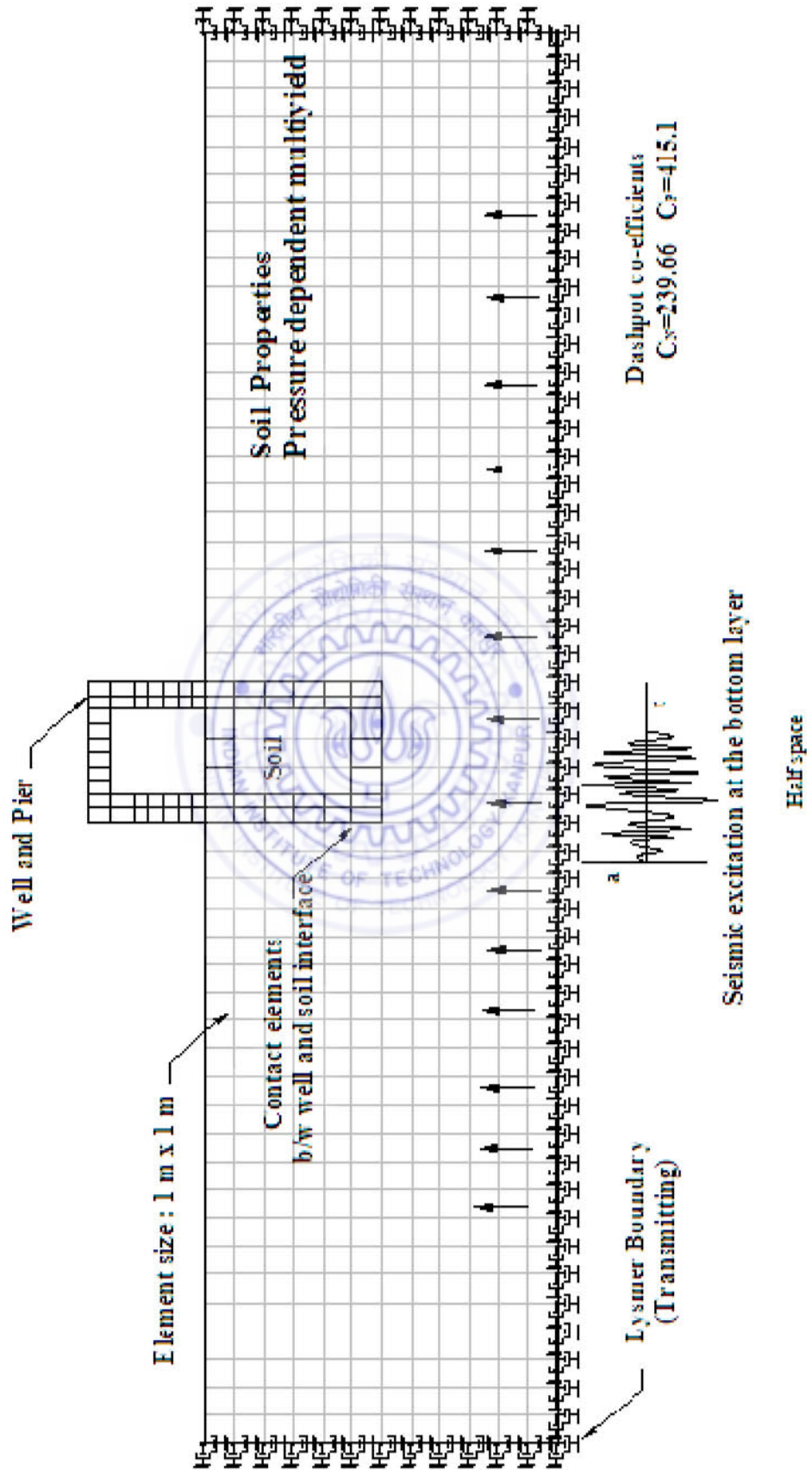
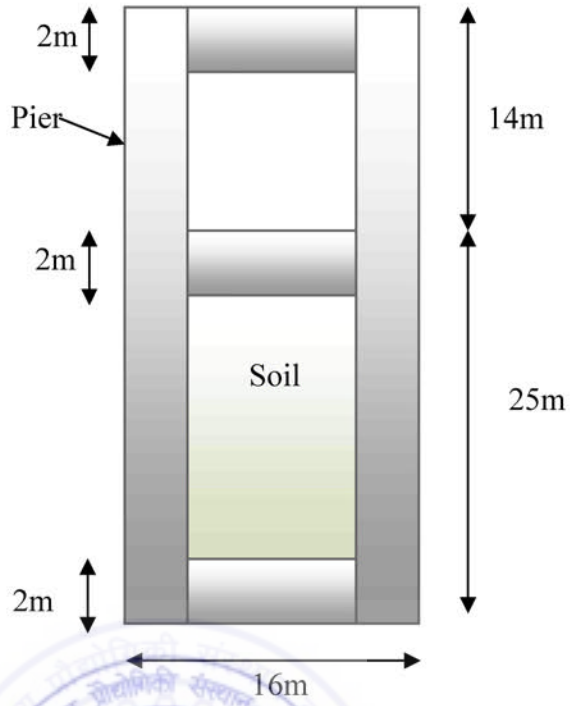


Figure 3.5: 2D- Soil –well- pier system with contact elements at soil-well interface



**Figure 3.6: Dimensions of Caisson and pier**

### 3.3 Observations from the Analysis

Figures 3.7-3.9 show comparison of the response spectra for the model at different locations. In Figure 3.6, the input motion is compared with the response at a soil node near top of the model with the embedded caisson conditions. It is evident from this Figure that there was significant amplification in the acceleration when the waves passed through the soil strata, which is similar to the observations made during free-field analysis. Figure 3.8 compares the response spectra from free-field analysis and the analysis of soil-caisson system. The dominant frequencies and peak acceleration value both showed a significant changed due to presence of the caisson. Although the presence of caisson showed overall amplification for most of the frequency content, the waves having time period lower than 0.25 amplified manifolds in the presence of caisson. The response spectra at the bottom and top of the well have been compared in Figure 3.9, which again shows considerable amplification and shift of dominant frequencies.

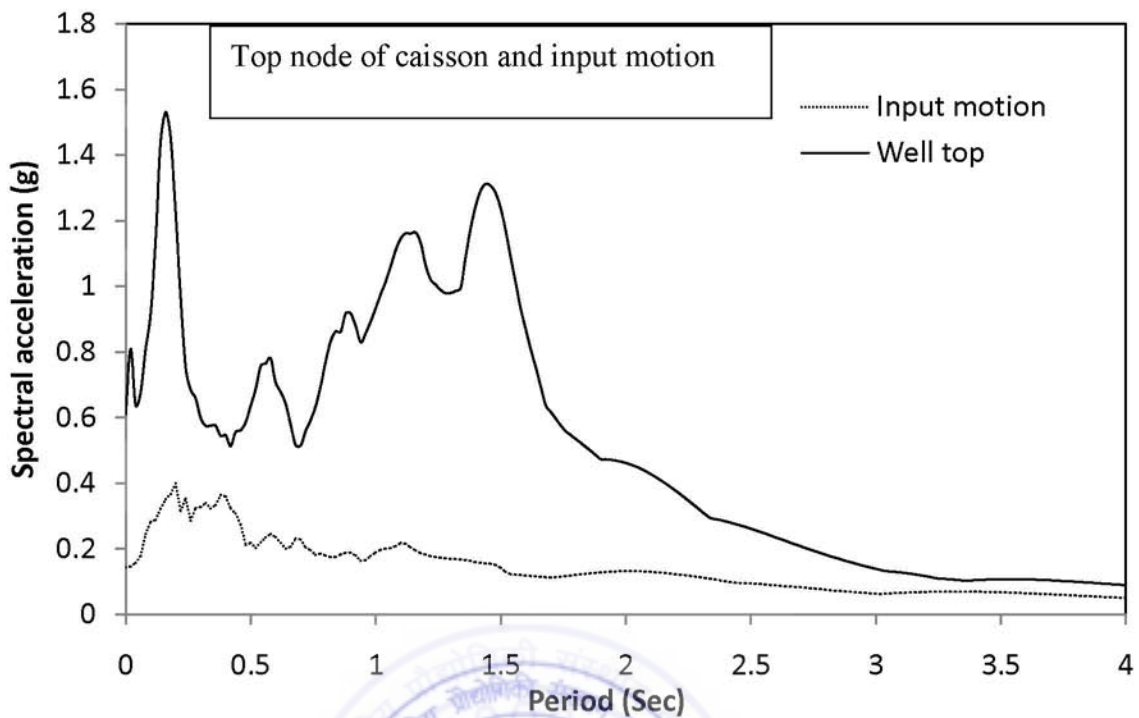


**Figure 3.7: Response spectrum between input motion and top of the well**

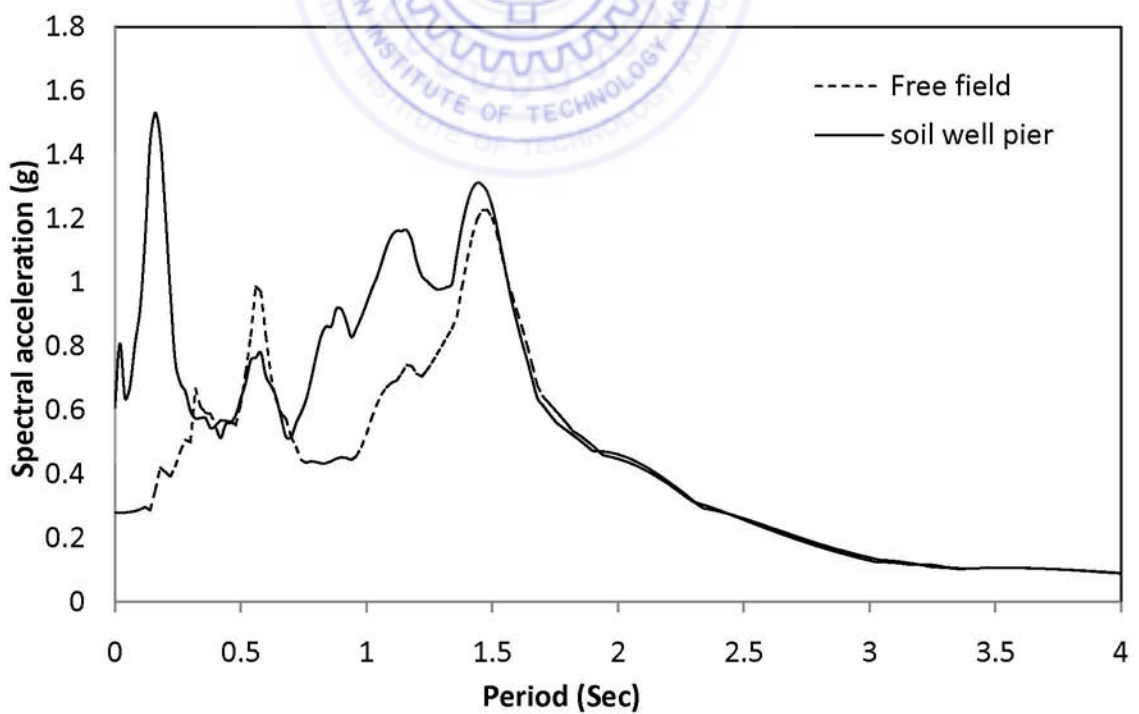


**Figure 3.8: Response spectrum at top node in free-field and soil-caisson system**

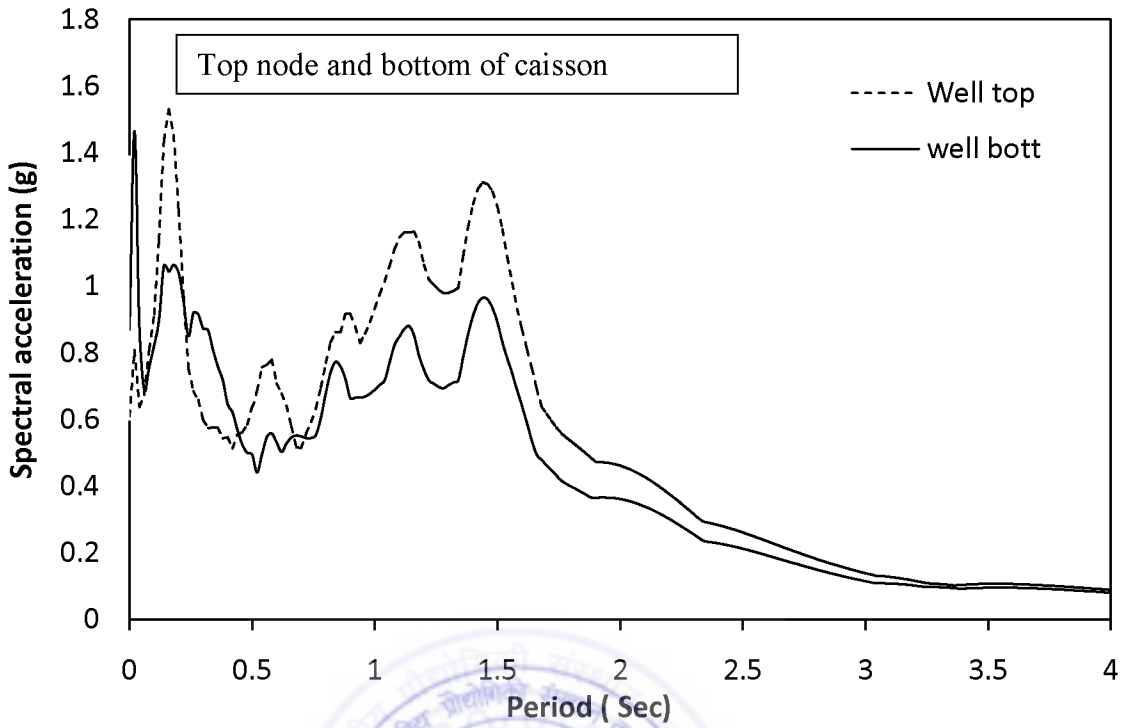


**Figure 3.9: Response spectrum at top and bottom of well**

### 3.4 Modeling slip and separation

In Finite element analysis, the situations often arise where discontinuous behavior occurs between finite elements such as interfaces between dissimilar materials and joints. The discontinuous behavior at the interface can be modeled using constraint equations or by connecting the elements with each other by discrete springs. Nodal compatibility of the finite element method constrains the adjacent structural and soil elements to move together. Particular advantages of using the interface elements are the ability to vary the constitutive behavior of the soil-structure interface and to allow differential movement of the soil and the structure, i.e. slip and separation. Incomplete contact between the foundation surface and the surrounding soil were taken into account by using contact spring model.

The interface properties between the caisson and the soil can have a dominating effect and must be accurately modeled in the analysis. The most appropriate way of doing this is to include interface elements within the mesh. There are several methods to model soil-

structure interfaces. Of these the use of the zero-thickness interface elements is probably most popular. The selection of normal and tangential stiffness of the interface elements is very important as very lower values dominate caisson behavior where as large values cause numerical ill-conditioning.

Figure 3.10 shows the displacement profile of caisson embedded in soil during transient analysis. It shows the separation along the bottom and side of caisson when subjected to seismic excitation. As the separation is relatively small in comparison to caisson dimensions, the displacements have been magnified in Figure 3.10 for the visualization purpose. The loss of contact between caisson and soil is clearly visible on one of the sides and bottom of the caisson. Such separation and gapping phenomenon can have significant impact on the observed response of the structure to the input motion as the stress distribution varies at the contact surface.

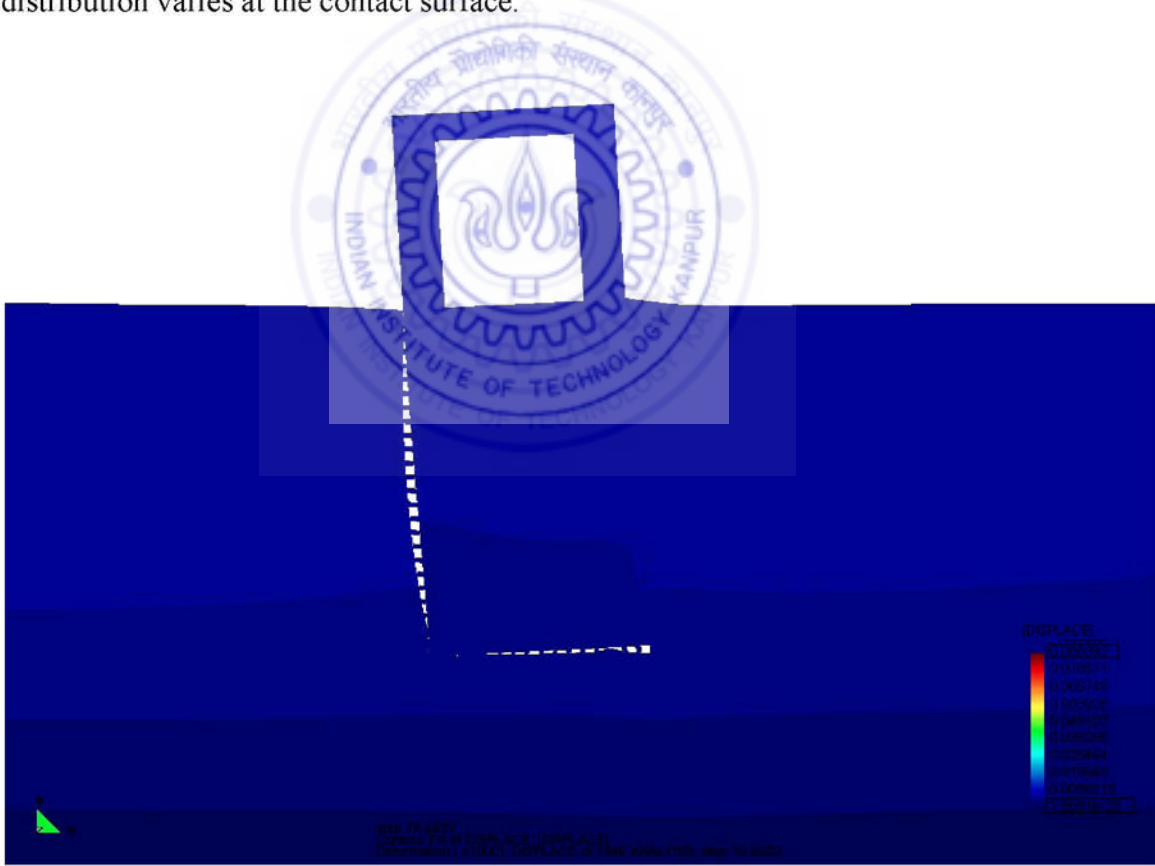


**Figure 3.10: Separation at the soil-Caisson interface**

### **3.5 Interference of shear waves**

After applying the seismic excitation at the bottom of the model domain, the wave propagates upwards in the subsequent time steps. As the wave propagation velocity depends on the stiffness of the materials the wave travels much faster in concrete than the surrounding soil. This phenomenon was observed during the initial time steps and two of such examples have been shown in Figure 3.11 and 3.12. The secondary waves generated by the caisson cause interference with the free-field vibrations of the soil as it reaches well before free-field vibrations at a particular point. This can be clearly observed from the figure 3.11 and 3.12 on the right side of the caisson. The intensity and zone of interference both increased in the subsequent time steps; and consequently, it became difficult to distinguish between the free-field waves and the waves transmitted through caisson. The effect of these caisson transmitted waves was observed around the caisson up to a certain distance. The region beyond this zone of influence had little effect of caisson and the response matched exactly with the free-field response. Hence, it becomes quite essential to study this zone of influence around the caisson in more detail using a quantitative approach so as to gain better understanding of the caisson response. Figure 3.8 shows the difference between the free-field and the soil caisson system as the response changes due to change in the natural frequency of the system.

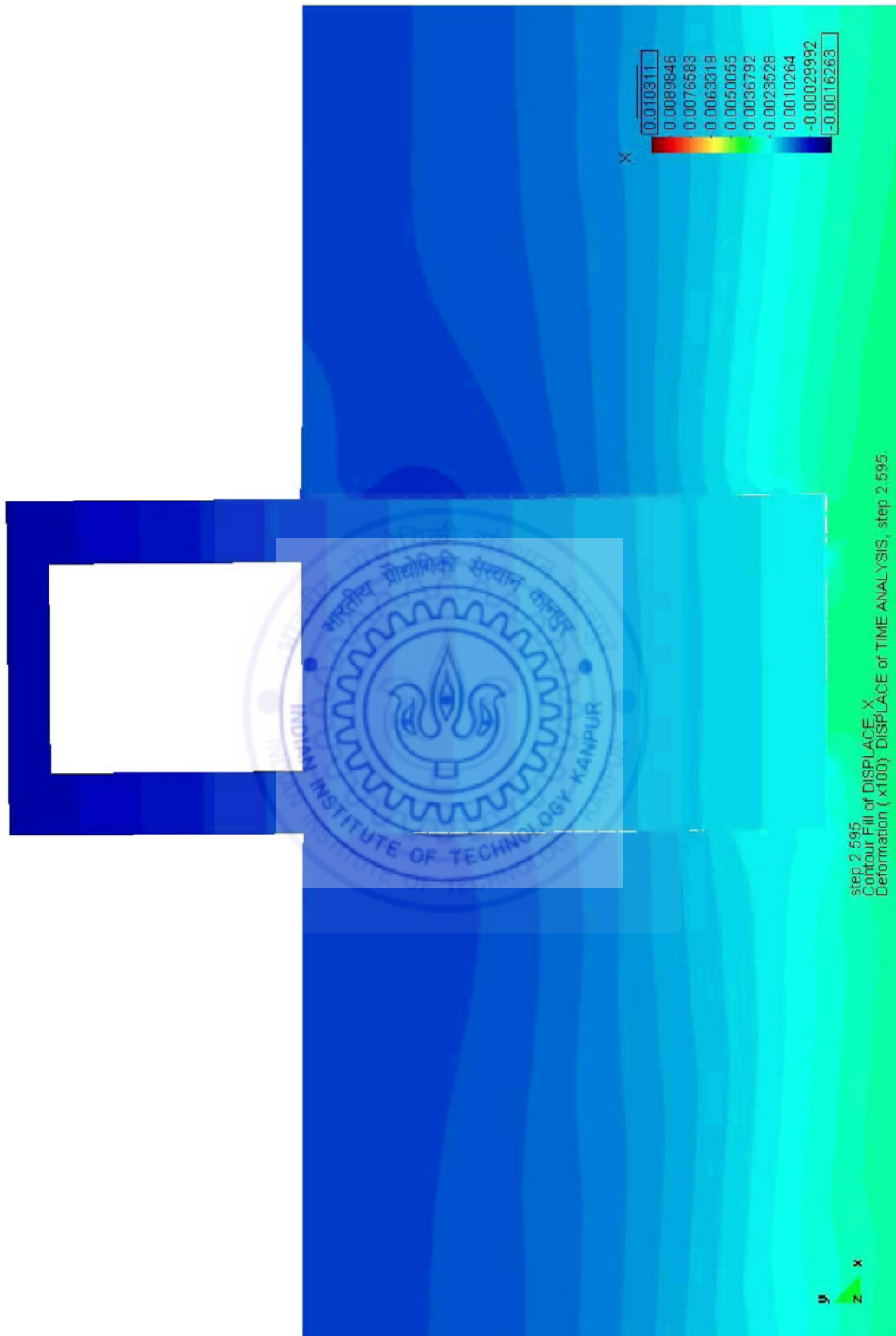


Figure 3.11: Interference of Shear waves

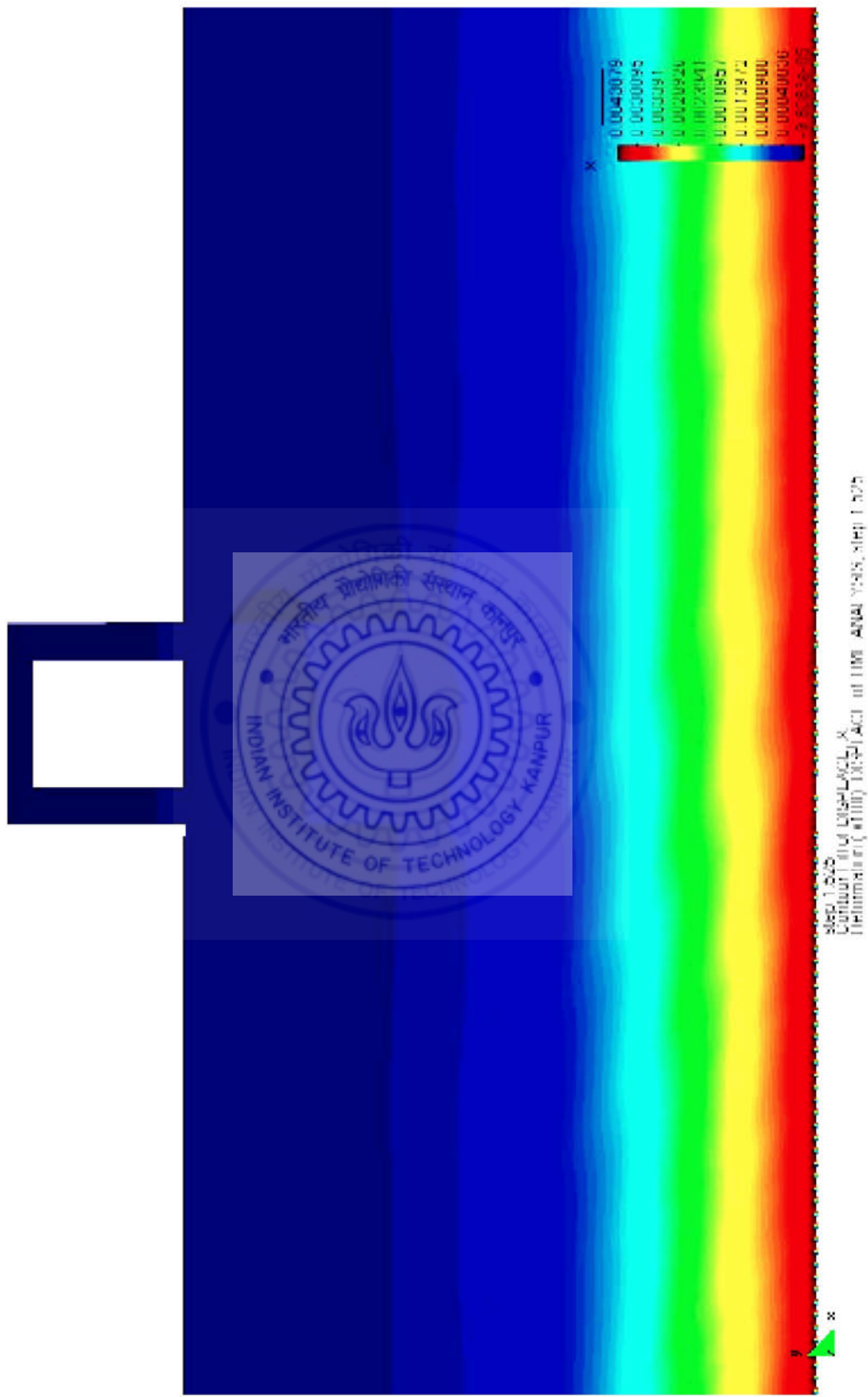


Figure 3.12: Wave propagation in the soil-caisson system

# CHAPTER 4

## INFLUENCE ZONE OF EMBEDDED CAISSON IN SOIL DOMAIN

---

The presence of adjacent structures can modify the state of stress within the ground and these effects must be accounted for in the analysis. As the response of soil-caisson is different from free-field it becomes imperative to study about the zone of influence around the caisson during transient loading. The term influence zone corresponds to the region where there is substantial influence of caisson on the response of the soil. For seismic analysis and design it is essential to study the influence zone around the structure. This gives an idea about the domain to be considered while designing, as analysis of a large domain is computationally expensive. Such a study also provides information about the magnitude of amplification/attenuation in the surrounding soil mass in the presence of embedded structure which is useful for design of the structure considering secondary aspects such as liquefaction. As most of the structural damage is due to the horizontal ground movements, horizontal acceleration response was considered in the present analysis.

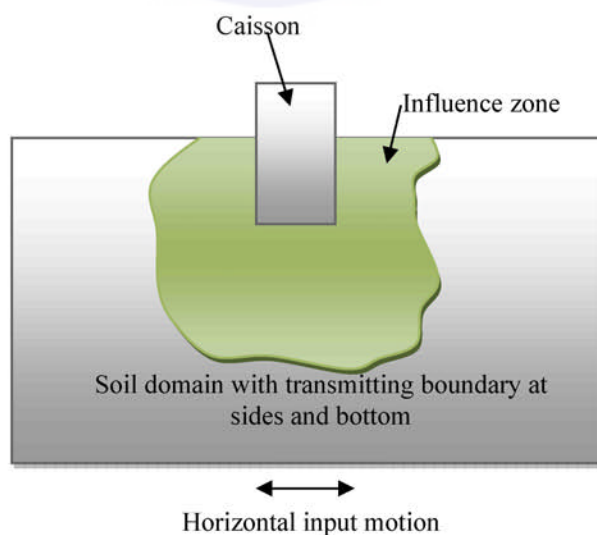


**Figure 4.1: Influence zone around caisson**

In order to study the effect of involving interface elements into the model and their effect on the interpreted influence zone, the analysis was performed for Soil-caisson with interface elements along the interface and Soil-caisson with rigid contacts along the interface.

## **4.1 Determination of the Zone of Influence Using Peak Acceleration**

Transient analysis of the soil-caisson model was performed for 4000 time steps. The most common way of describing a ground motion is with the displacement/acceleration time-history at different nodes in the model. Many parameters have been proposed to characterize the amplitude, frequency content and duration of strong motions. Peak acceleration, peak velocity and peak displacement are amplitude parameters of ground motion. As peak horizontal acceleration is the most commonly used measure of amplitude of a particular ground motion which is the maximum value of acceleration from the accelerogram. As the largest dynamic forces in case of stiff structures are induced due to the peak horizontal acceleration this is used as a common amplitude measure.

### **4.1.1 Generating Contour Plots for Variation of Peak Accelerations**

The response obtained from free-field and soil-caisson models were used for the calculation of peak horizontal accelerations at the specified nodes in a horizontal and vertical grid dimension of 4 m and 5 m respectively. The ground motion parameters at all the grid points were calculated using Seismosoft software. The X and Y co-ordinate denote the location of the node in the soil mass with respect to the face of well on one side. The relative change in peak horizontal acceleration from free-field analysis to the analysis of soil-caisson system at a node was normalized by the value of peak acceleration from free-field response at the same node. This can be denoted by a non-dimensional parameter  $\zeta_p$  as shown in the equation below.

$$\zeta_p = \frac{PHA_{SC} - PHA_{FF}}{PHA_{FF}} \times 100 \quad \dots \quad (4.1)$$

Where  $PHA_{SC}$ ,  $PHA_{FF}$  are PHA acceleration corresponding to soil-caisson system and free-field analysis respectively.

The value of non-dimensional parameter  $\zeta_p$  in percentage was then used to plot the contours of its variation in soil domain as shown in Figure 4.2. As the domain is symmetric about the vertical-axis, the contours have been shown for only one side of the caisson i.e. the left half of the model.

#### **4.1.2 Interpretation from the variation of peak acceleration contour**

The contour plot shown in Figure 4.2 gives the variation of the peak horizontal acceleration (PHA) in the analysis of soil-caisson system with respect to the free-field analysis in the form of a non dimensional parameter  $\zeta_p$  described in equation 4.1. This figure shows that there was a significant variation in peak acceleration at the top surface ranging up to 20 m away from the caisson face. One should note here that the maximum change in peak acceleration was observed at around 16 m away from the caisson and not close to the caisson face. There was not much variation of PHA observed at depth below 15 m from the ground surface.

Since the information of the variation of PHA does not include the variation in frequency content, the interpretation of influence zone was not complete. Figure 4.3 shows the response spectra at a node 4 m away from the caisson face and at the ground surface. These response spectra show no significant variation in the PHA values but the frequency content was much different for free-field and soil-caisson system. Similar observations were made for the nodes at 15 m depth and below. Hence, it is evident that comparing the PHA alone does not give accurate interpretation of influence zone for such problems. The change in frequency content was mainly due to the interference of secondary waves with the free field motions near the caisson.

Figure 4.4 shows the response spectrum at the ground surface which was 24 m away from the caisson face. As the frequency content matches closely between both the analysis, PHA can be used in this case. Hence it becomes evident that frequency content as well as amplitude should be considered while analyzing, and PHA alone cannot be used in this case to evaluate the influence zone where frequency content is bound to different.

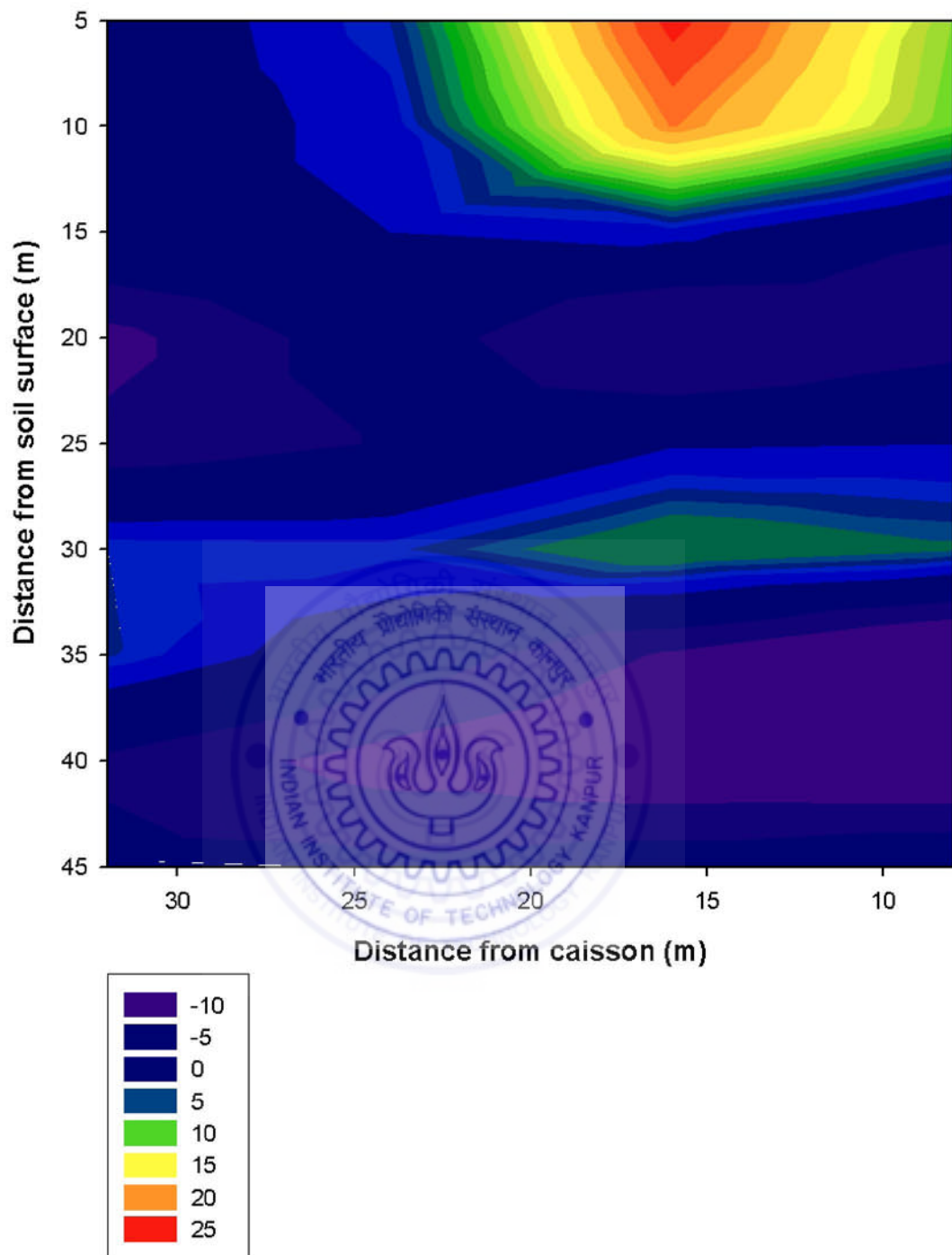


**Figure 4.2: Contour for the relative change in peak horizontal acceleration**

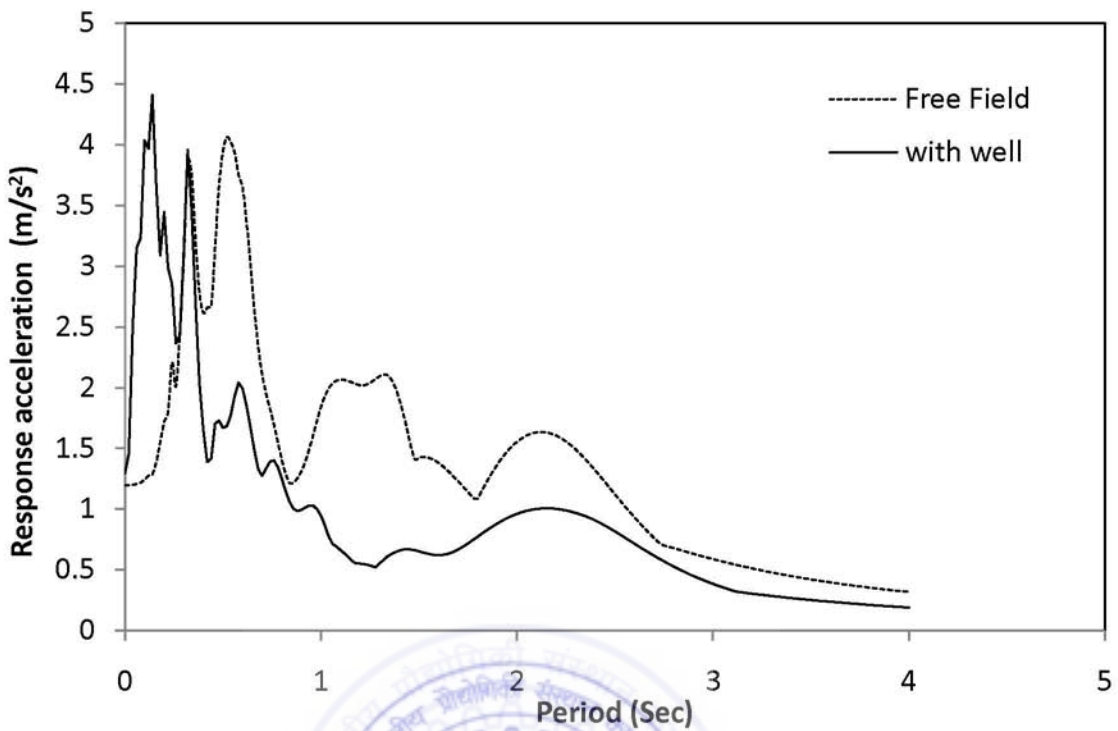


**Figure 4.3:** Response spectrum at a 4 m away from caisson at top

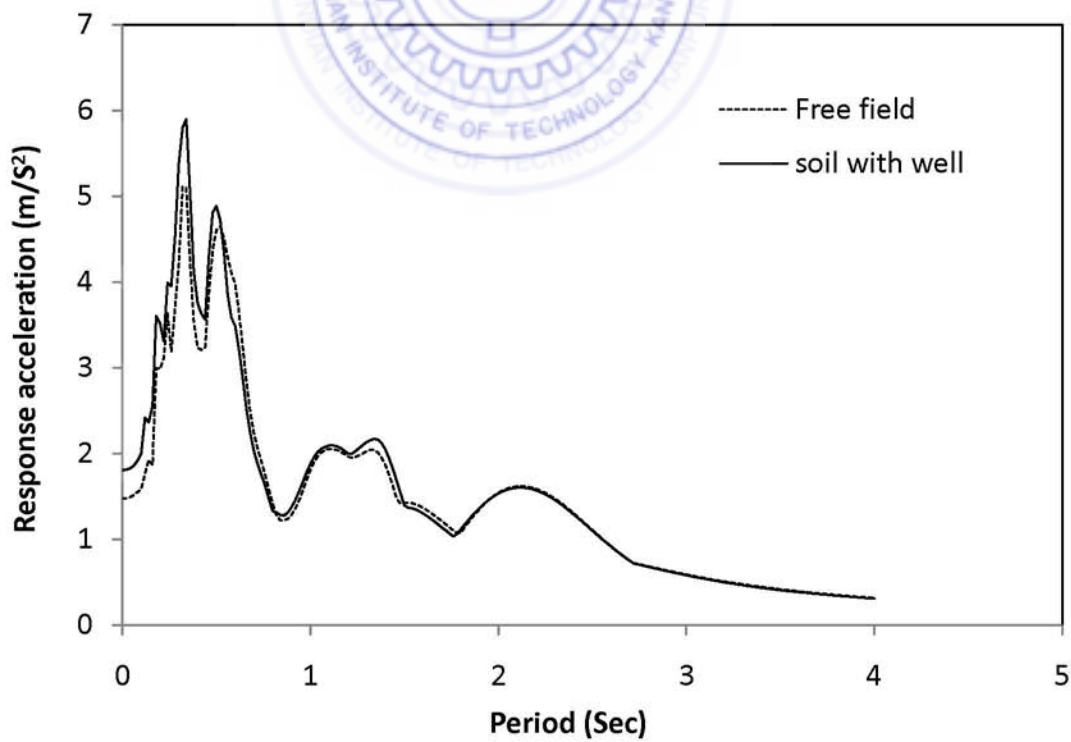


**Figure 4.4:** Response spectrum at a 24 m away from caisson at top

## 4.2 Determination of the Zone of Influence Using RMS Acceleration

Earthquakes produce complicated loading with components of motion that span a broad range of frequencies. This frequency content describes how the amplitude of a ground motion is distributed among different frequencies. Since the frequency content of an earthquake motion will strongly influence the effects of that motion, characterization of the motion cannot be complete without consideration of its frequency content. Therefore, a single parameter that includes the effects of amplitude and frequency is to be obtained for the data comparison. As discussed in the section 2.4, the RMS acceleration can be used in this type of study as it contains information about the amplitude as well as the frequency content. The RMS values were determined at required nodes for the evaluation of influence zone. Similar to the exercise performed to study the variation of PHA, the contours plot was generated for the variation of the change in RMS acceleration from the free-field analysis to the analysis of soil-caisson system by defining another non-dimensional parameter  $\zeta_R$  as given below.

$$\zeta_R = \frac{RMS_{SC} - RMS_{FF}}{RMS_{FF}} \times 100 \quad \dots \dots \quad (4.2)$$

Where  $RMS_{SC}$  is RMS acceleration corresponding to soil-caisson system

$RMS_{FF}$  is the RMS acceleration corresponding to free-field analysis

### 4.2.1 The Influence Zone of Embedded Caisson with Contact Elements

Figure 4.5 shows that the variation of the non-dimensional parameter  $\zeta_R$  is below 10% after a distance of 20m from the caisson periphery. This is the zone around the caisson that the effect of rigid caisson was observed. Figure 4.6 shows the variation of RMS acceleration with distance from the well for different depths from the soil surface. Figure 4.7 shows the percentage variation of RMS acceleration with distance from the well for different depths. The percentage variation was less than 10 % from a distance of 20 m from the caisson. The response spectrum between the free-field and soil-caisson coincides after this zone of influence of 20 m. Appendix 5 shows the influence zone contour with smaller contour interval as 10 % variation cannot be visualized from figure 4.5.

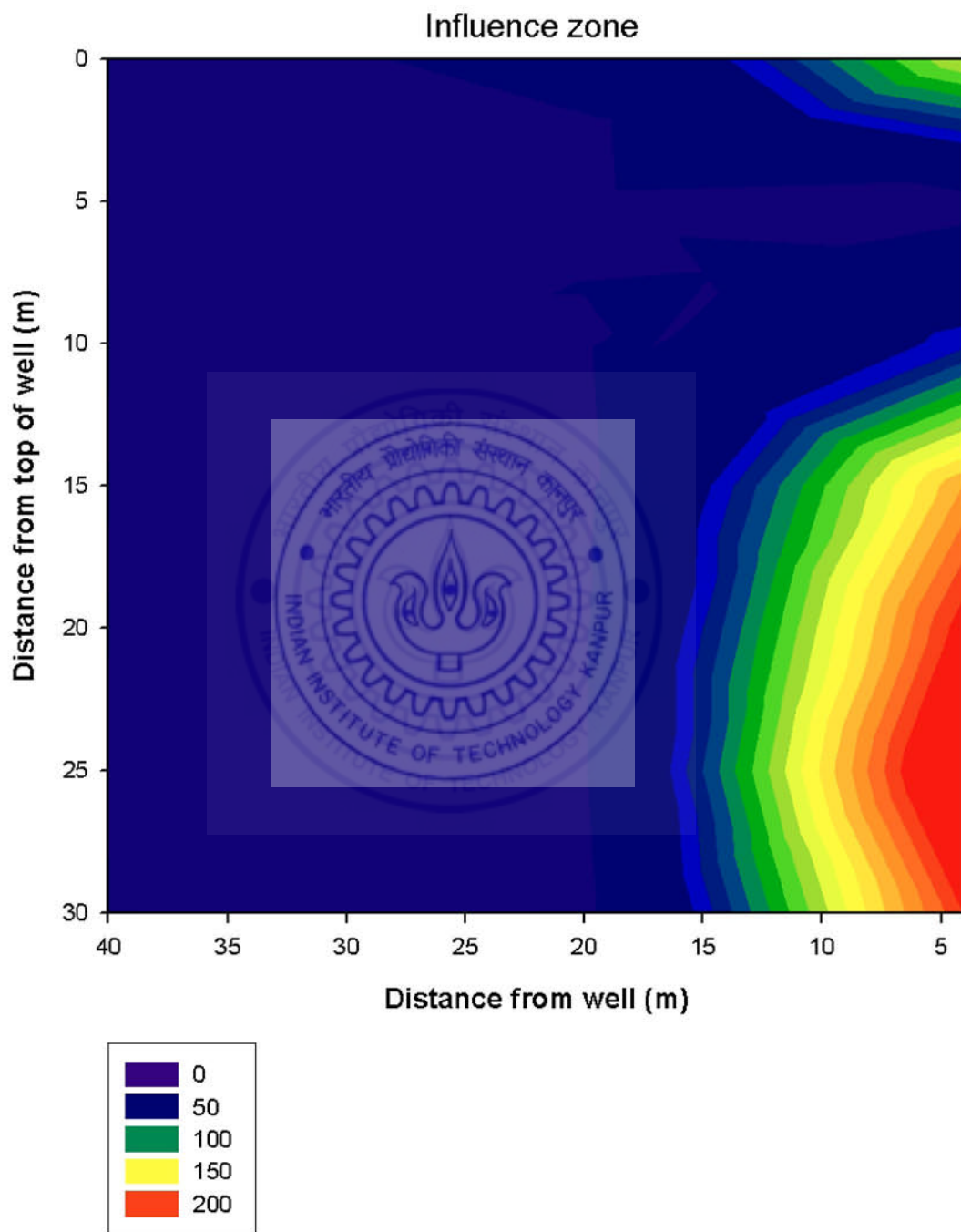


**Figure 4.5: Influence zone for soil-caisson with contact elements along the interface**

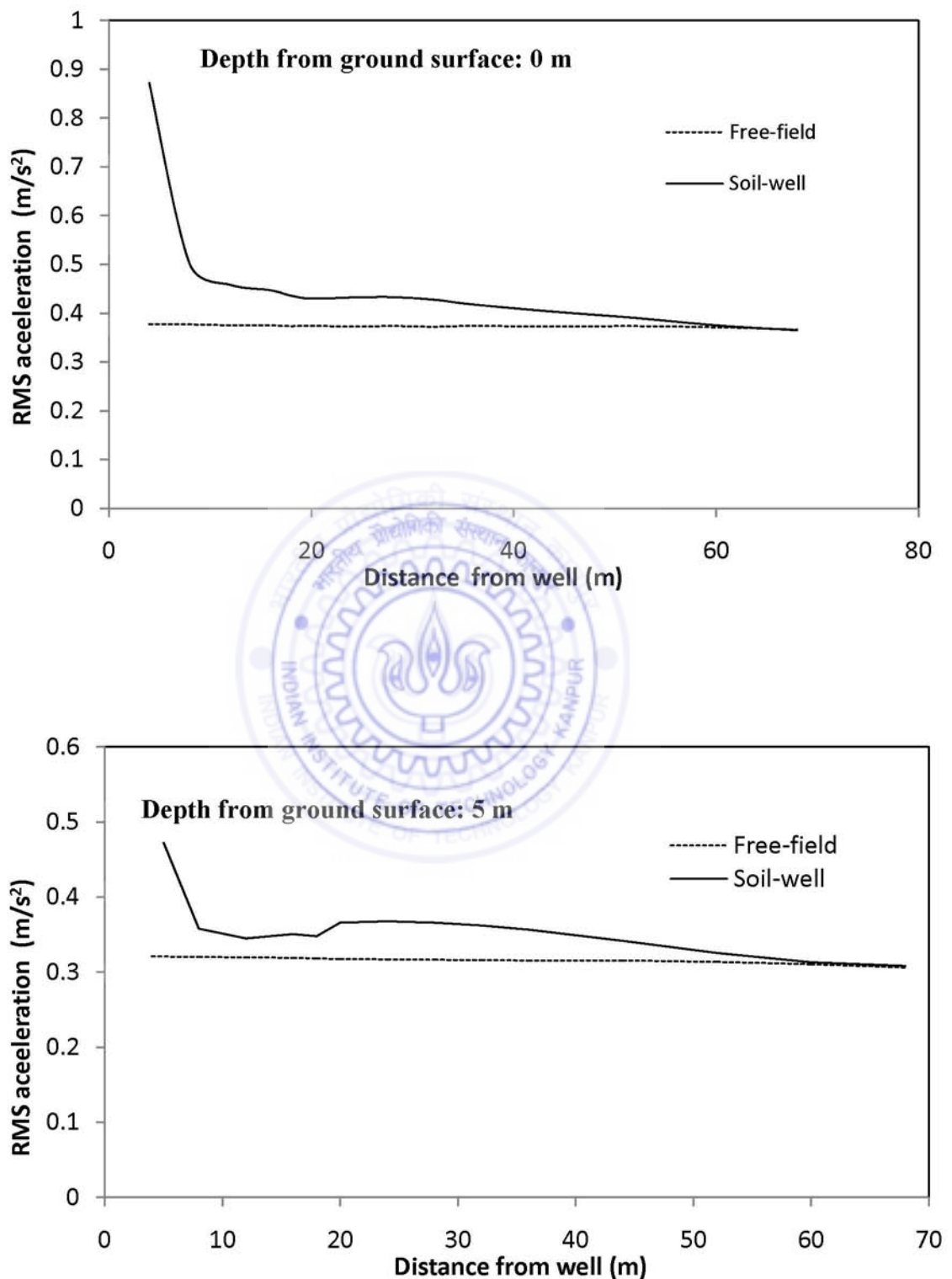


**Figure 4.6: Variation of RMS acceleration with depth from the ground surface**

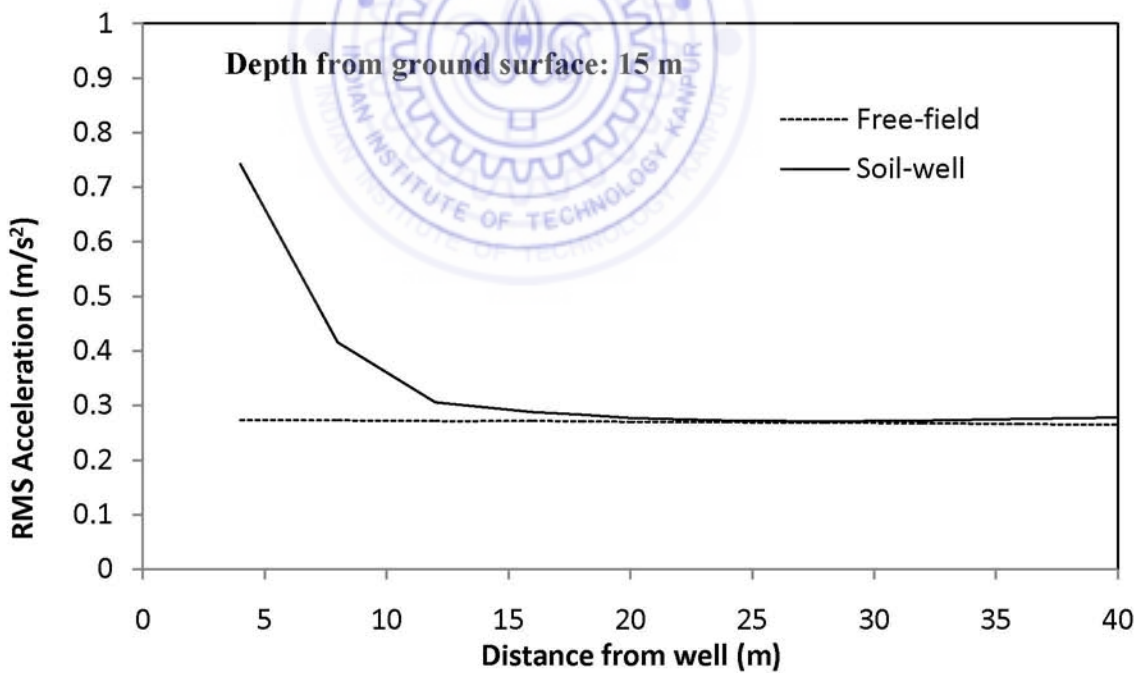
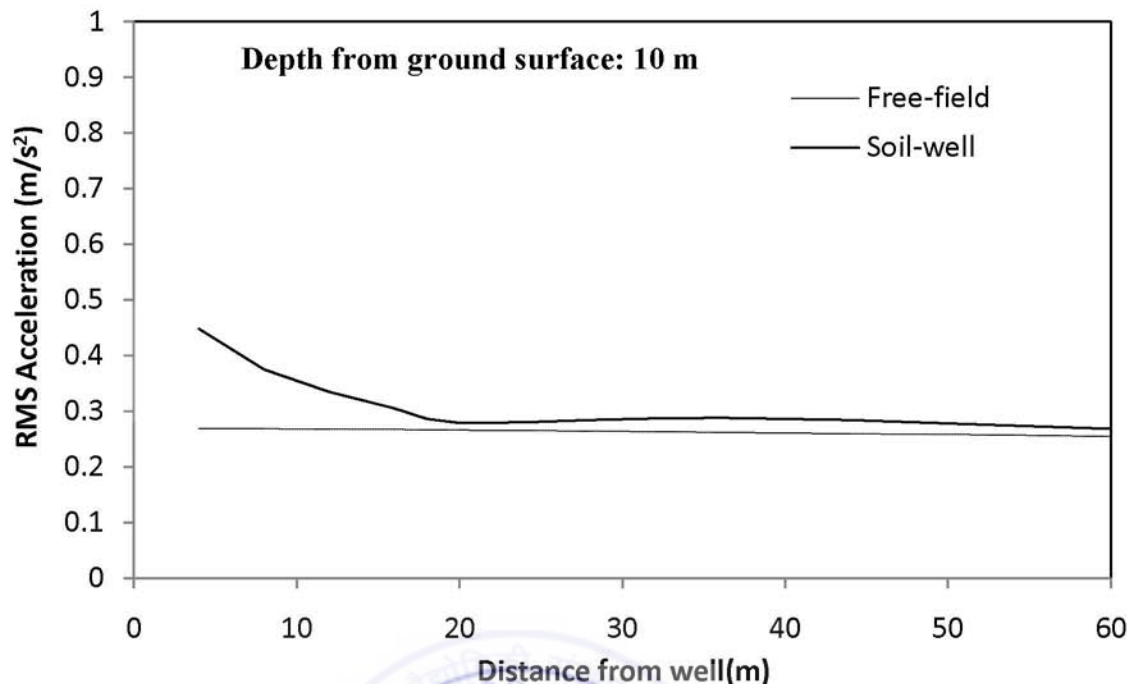


**Figure 4.6: Continued.**

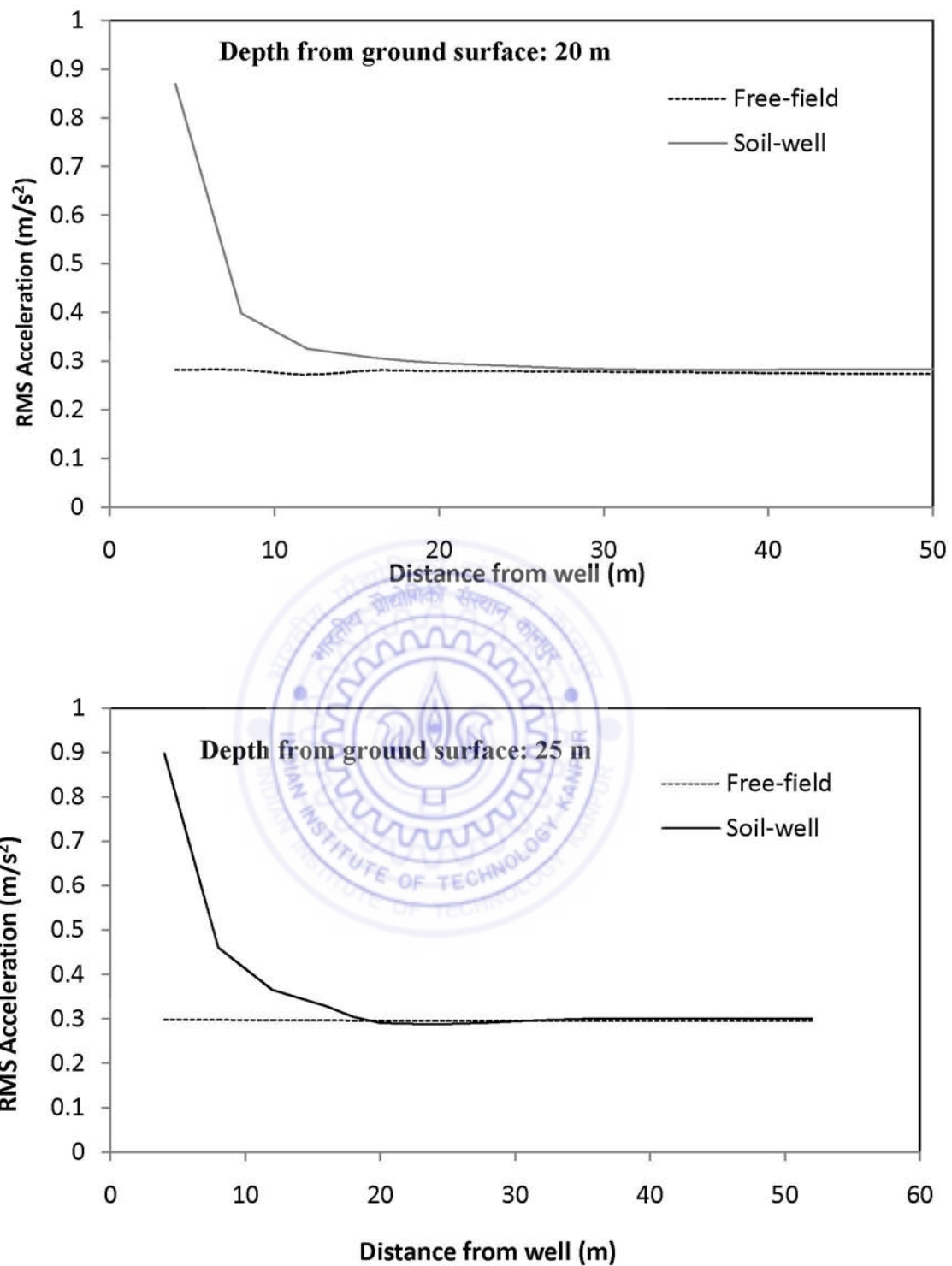


Figure 4.6: Continued.

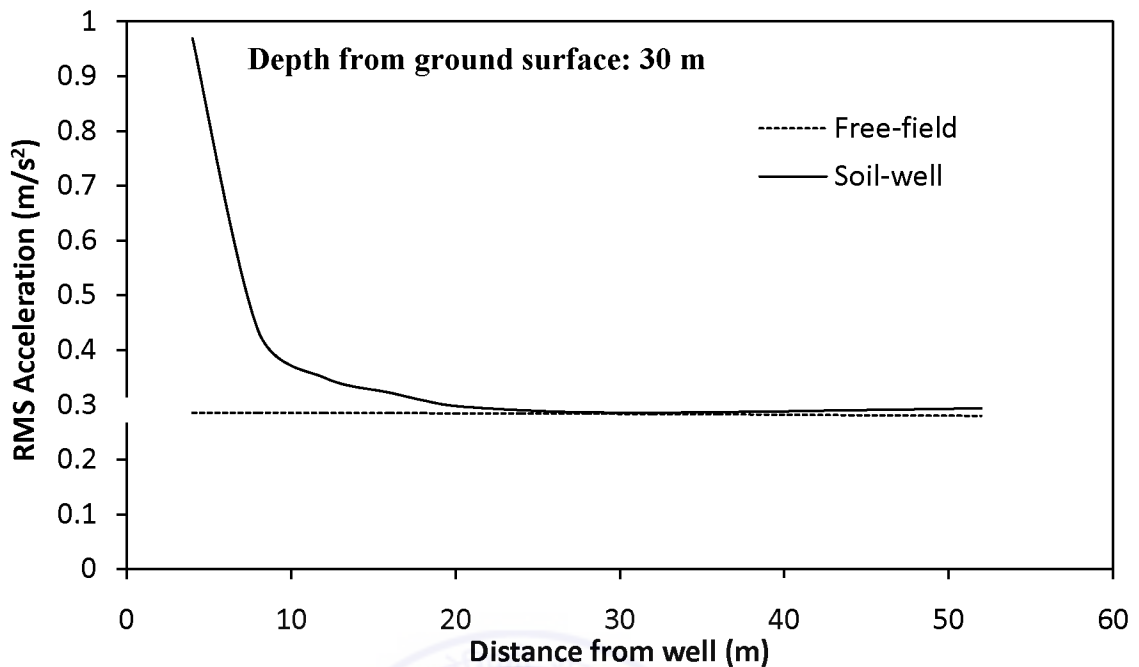


Figure 4.6: Continued.

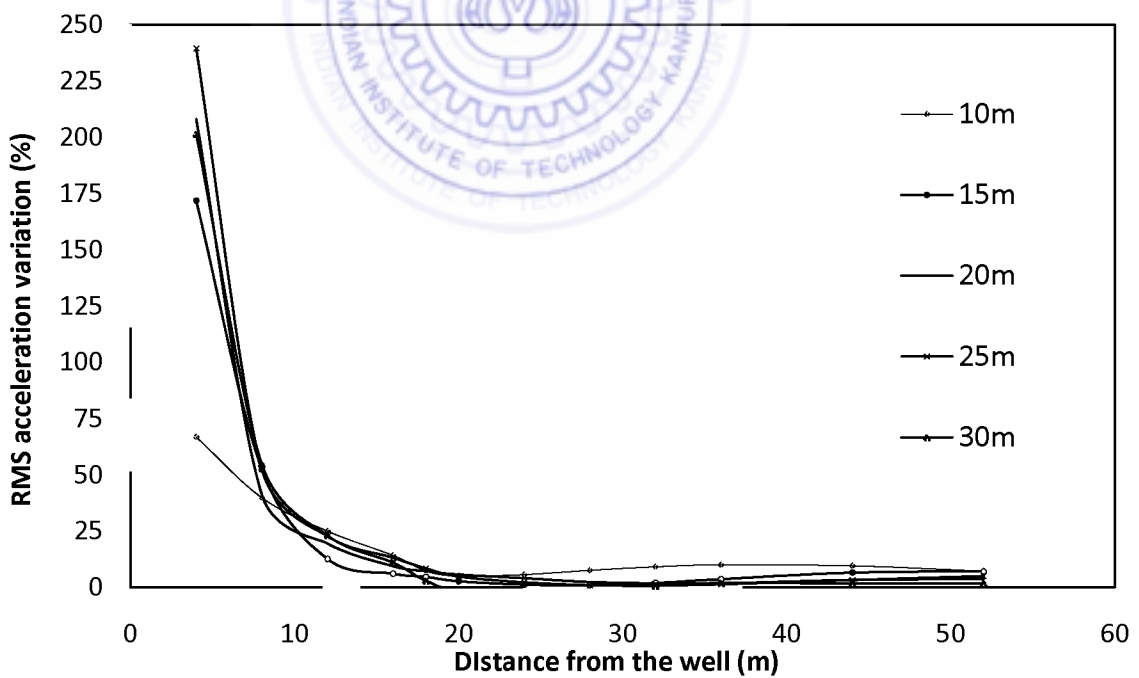
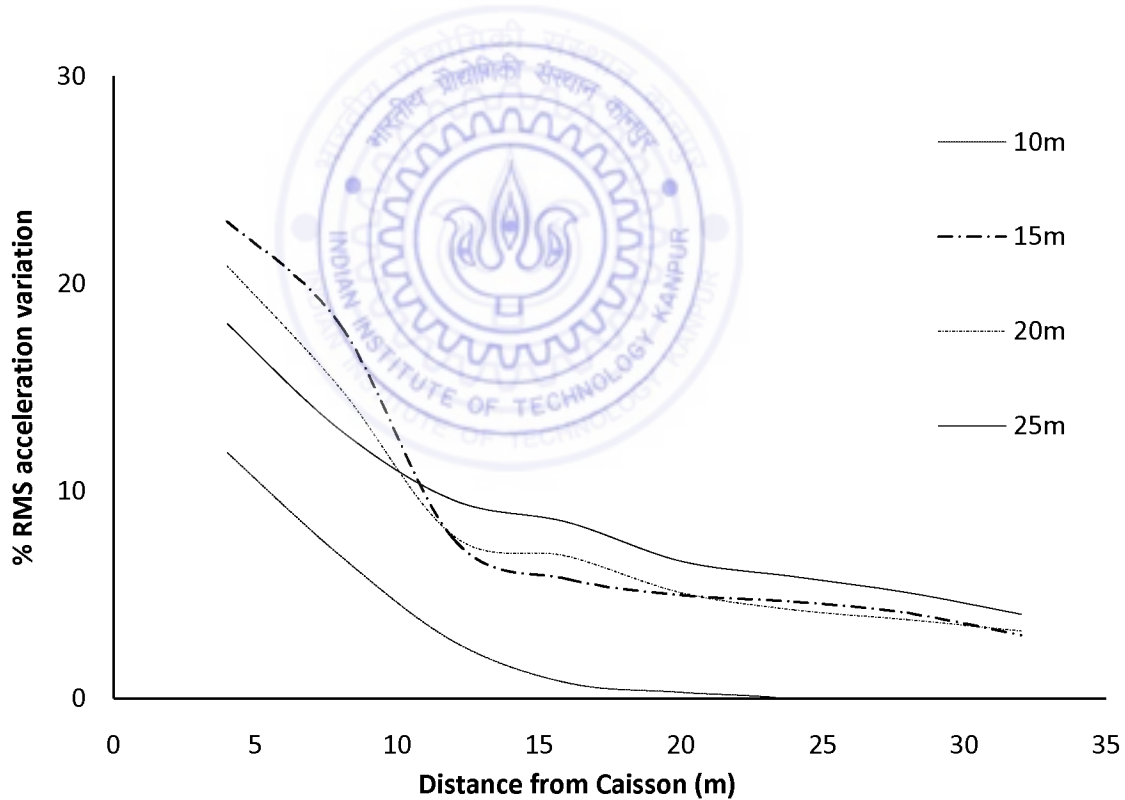


Figure 4.7: Percentage variation of RMS acceleration from Free-field to Embedded Caisson condition

#### 4.2.2 The Influence Zone of Embedded Caisson with Rigid Contacts

The study was performed without contact elements at soil-caisson interface, keeping all the other model parameters similar to the previous model described in section 4.2.1. Figure 4.8 shows the contour plot of variation of non-dimensional parameter  $\zeta_R$  with the horizontal distance from the caisson periphery. It can be observed that the variation is less than 10 % from a distance of 15 m from the caisson periphery. Figure 4.9 also shows the percentage variation of  $\zeta_R$  with distance. This concludes that the free-field response matches with the soil-caisson system beyond the zone of influence. There is significant variation at the top 10 m from the soil surface.



**Figure 4.8: Variation of RMS acceleration with distance from the caisson Embedded Caisson with Rigid Contacts with soil**

## Influence zone

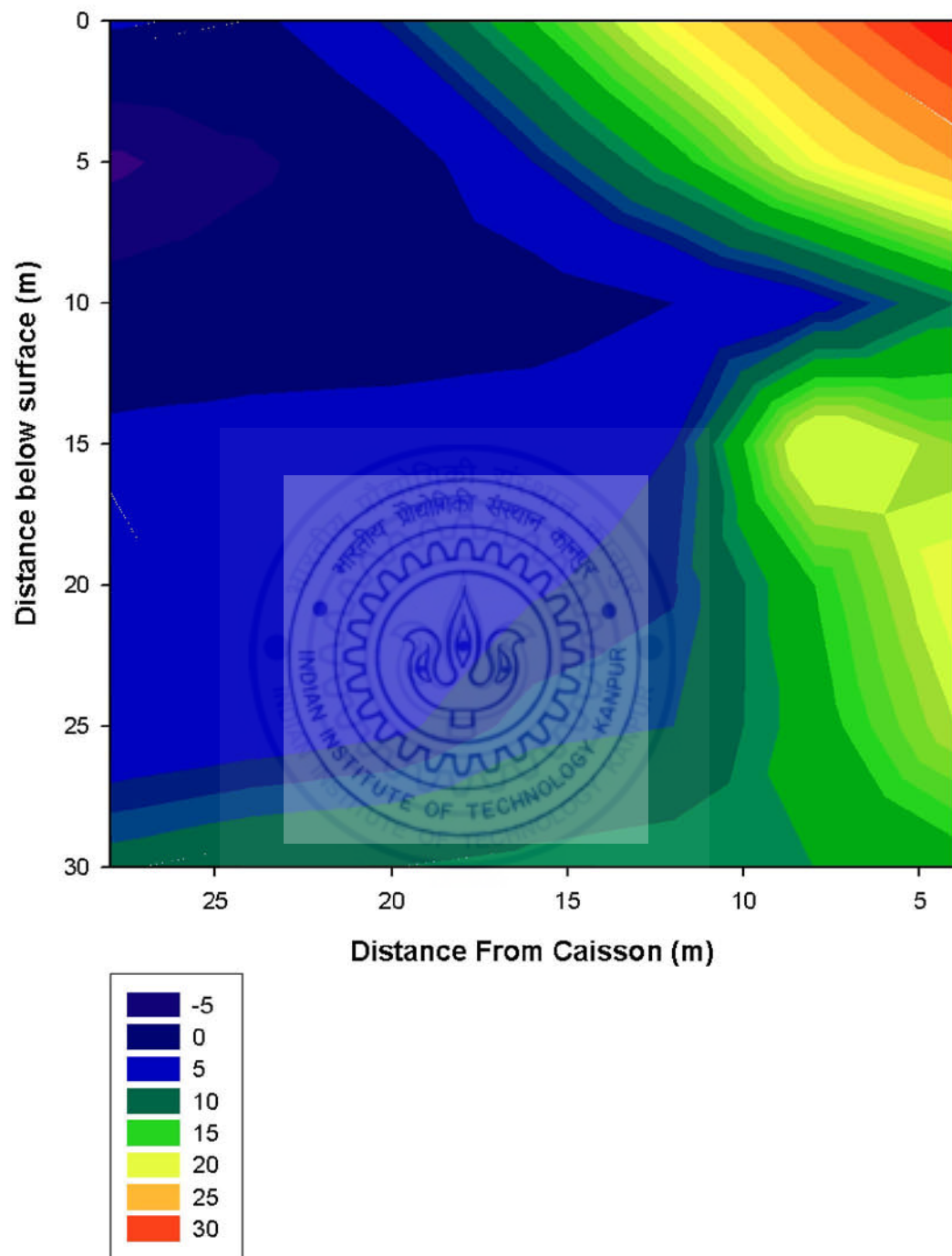


Figure 4.9: Variation of RMS acceleration with distance from the caisson for case: 1

### **4.3 Summary of Observations from Influence Zone Study**

Figure 4.7 and 4.8 shows the contour of variation of  $\zeta_R$  with distance from the caisson periphery. As the soil-structure interactions have pronounced affects on the response of the whole system the influence zone in both the cases are different. The influence zone with rigid contacts is 15 m where as analysis with contact elements have shown an influence area of 20m. There was significant variation of the RMS acceleration values in both the cases. The variation of the parameter  $\zeta_R$  is 35 to 40 percent near the caisson in the model with rigid contacts between the soil-caisson interfaces. However this variation is more than 100 percent in the model with contact elements at the interface. This was observed as the stress distribution changes when there is separation along the interface. This phenomenon is due to the reflections, refractions of the waves at the interface of two dissimilar materials. These reflection and refraction of the waves is mainly due to change in the material properties (stiffness). Appendix 6 shows the response spectra obtained at a distance of 20 m from the caisson periphery. The response spectra match between the free-field analysis and the soil-caisson system. This proves that the frequency content matches with free-field response for the soil-caisson (interface elements) beyond the influence zone.

# CHAPTER 5

## SUMMARY AND CONCLUSIONS

---

### 5.1 Summary and Conclusions

The effects of soil-structure interaction are often ignored while performing seismic analysis conventionally. Some procedures convert the dynamic problem into an equivalent static problem by applying certain correction factors. Some international codes, however, have provisions for modeling of soil springs for taking soil foundation interaction into account. The stress distribution changes significantly when soil structure interaction effects are considered. Presence of stiff structures like caissons can affect the surrounding soil up to an influence zone around the caisson and this zone of influence can be particularly of interest when two caissons are adjacent to each other. If the distance between adjacent caissons is small (within the zone of influence of one of the caissons) then there will be effect of adjacent caissons and it contributes to the response significantly. Several other secondary effects such as Liquefaction around the caisson may also be studied once some understanding of the influence zone is developed. The present study focused on the behavior of single caisson of 25 m length embedded in uniform soil strata with rock bed at 50 m depth. Two-dimensional transient dynamic analysis was performed considering various aspects related to soil-caisson interface, boundary conditions, etc. The influence zone of embedded caisson was studied quantitatively considering peak horizontal acceleration and RMS accelerations. This study can be concluded with the following key observations.

- Element dimensions that are too large may filter out high frequencies whereas very small element divisions can introduce numerical instability and require huge computational resources. Considering a balance between these two constraints, the element dimensions must be calculated by considering the lowest velocity of

the mechanical wave in existing soil media (Rayleigh wave velocity).

- The time-step for the transient analysis should not be less than one-tenth of smallest fundamental Time-period of the system as it affects the numerical stability and accuracy of the analysis. Time steps larger than the fundamental frequency of the system may diverge the solution and can lead to erroneous interpretations.
- The treatment of transmitting boundary becomes significant as no waves should be reflected back in to the computational domain. The Lysmer transmitting boundary was used in this study along the sides and the bottom of soil domain, which was found successful in minimizing the wave reflections.
- Damping is a complex phenomenon and the parameters defining the damping should be carefully selected. The frequency dependent Rayleigh damping parameters were used in this study, which were determined considering the frequency content of input motion.
- The use of zero-length contact element (compression only material) at the soil-caisson interface showed relative slip and separation during the transient analysis. The parameters such as stiffness should be selected carefully in case of the zero-length elements in order to avoid computational difficulties due to high stress gradients.
- The response of the soil-caisson system is affected due to the secondary waves generated by the caisson to the soil domain as the wave velocities are higher in concrete than soil due to high stiffness. Hence these waves develop secondary waves that propagate in to the soil domain and change the free-field response significantly up to certain region which could be called as the zone of influence.
- The peak horizontal acceleration does not reflect the frequency content of the ground response. Hence, ground motion parameters that incorporate amplitude as well as frequency content have to be selected for the evaluation of influence zone around the caisson. The RMS acceleration was used in this study to evaluate the influence zone of the embedded caisson.
- The influence zone around the caisson increased in area when the analysis was performed with contact elements in comparison to the rigid contacts.

- At 4 m distance from the caisson face, there was around 130 percent increase in RMS acceleration values for soil-caisson system in comparison to the free-field and analysis when the contact elements were used at the interface. When the soil-caisson interface was taken as rigid, there was only 35 to 40 percent increase in the RMS acceleration around the caisson periphery. The influence zone for the 16 m diameter caisson was observed to be extending up to 20 m and 15 m respectively in the case of compression only contacts and rigid contacts.

## 5.2 Scope of Future Research

- In the present study, two-dimensional analysis was performed assuming plane strain conditions to evaluate the influence zone of embedded caisson. This study can be extended by performing three-dimensional analysis to evaluate the influence zone of embedded caisson more accurately. Such an analysis can also facilitate study of the effect of various shapes and sizes of the caissons.
- This study considered pressure dependent elastic material for the soil mass. However, the soil is known to be highly non-linear material. The model developed in this study can be easily extended to incorporate non-linear material models to study the behavior of embedded caissons.
- The depth of caisson was taken as half of the depth of rock bed in this study. A similar study can be performed to study the behavior of caissons resting on rock bed. To develop a realistic model of the contact between the rock bed and caisson will be the challenge in this study considering the fact that the transient loading is to be applied at the rock bed itself. Another case which can be taken up for study is the behavior of a short caisson (similar to a shallow foundation) embedded in a soil mass with rock bed at large depth.
- The bridges in India often use two caissons side-by-side as foundations of double carriageways. A model similar to the one in this study can be easily developed to study the interaction these neighboring caissons.
- A parametric study can be performed for the heterogeneity of soil mass, which may significantly affect the influence zone of embedded caisson.

- The above studies can be concluded to develop a realistic design methodology for caissons with due consideration to the seismic effects.



# References

- 1) Gerolymos N, and Gazetas G. (2006) , “Winkler model for lateral response of rigid caisson foundations in linear soil,” *Soil Dynamics Earthquake Engg.*, Vol. 26, pp. 347- 361.
- 2) Gerolymos N and Gazetas G. (2006) , “ Development of Winkler model for static and dynamic response of caisson foundations with soil and interface nonlinearities,” *Soil Dynamics & Earthquake Engg*, Vol. 26, pp 351-362
- 3) Gerolymos N and Gazetas G. (2006), “Static and dynamic response of massive caisson foundations with soil and interface nonlinearities , validation and results,” *Soil Dynamics Earthquake Engg*, Vol. 26, pp 377- 394.
- 4) Kramer S (1996), “Geotechnical earthquake engineering”. *Englewood Cliffs, NJ:Prentice-Hall*
- 5) Tassoulas JL (1981), “Elements for the numerical analysis of wave motion in layered media”,
- 6) *Research Report R81-2, Department of Civil Engineering, Massachusetts Institute of Technology, Cambridge.*
- 7) R. A Day and D M Potts (1994), “Zero thickness interface elements – Numerical stability and application,” *International journal for numerical and analytical methods in Geo-mechanics*, Vol 18, 689-708.
- 8) Chongbin zhao and S Vallappan (1993), “A dynamic infinite element for 3-dimensional infinite domain wave problems,” *International journal for numerical methods in Engineering*, vol 36, 2567-2580.
- 9) G. Beer (1985), “An isoparametric joint/ interface element for Finite element analysis “, *International journal for numerical methods in Engineering*, vol 21,585-600
- 10) Makris N and Gazetas G (1992),” Dynamic pile–soil–pile interaction. Part II, Lateral and seismic response”, *Earthquake Engg Structural Dynamics*,vol :21, pp:145–162.
- 11) Anastasopoulos I, Gerolymos N, and Gazetas G (2001), “Possible collapse

- reasons of an access span of the nishinomiya-ko bridge: kobe1995”, *Proceedings ofthe fourth hellenic conference on geotechnical engineering, Athens*, vol.2, pp: 83–90.
- 12) Mylonakis G (2001),” Elasto-dynamic model for large-diameter end-bearing shafts”, *Soil Foundations* Vol :41(3),pp: 31–44.
  - 13) Potts D.M and Fourie A.B (1986),” A numerical study of the effects of wall deformation on earth pressures”, *International journal numerical Anal. Geomech.*, Vol.10, No.4 pp 383-405
  - 14) Saitoh M.(2001),” Effective seismic motion of caisson and pile foundation”, *RTRI Rep* 46.
  - 15) Tajirian FF and Tabatabaie M.(1985),” Vibration analysis of foundations on layered media”
  - 16) Gazetas G and Selig ET, editors. “Vibration problems in geotechnical engineering” New York: ASCE.
  - 17) Zerwer A, Cascante G and Hutchinson J (2002), “Parameter Estimation in Finite Element Simulations of Rayleigh Waves”, *Journal of geotechnical and geoenvironmental engineering*, Vol: 128 No:3, pp 250-261
  - 18) Lysmer J, Kuhlemeyer L (1969), “Finite dynamic model for infinite media”, *Proceedings of ASCE*, Vol:95 No. EM4
  - 19) Youssef, Duhee Park (2002), “Viscous damping formulation and high frequency motion propagation in non-linear site response analysis”, *Soil dynamics and earthquake engineering* Vol:22, pp 611-624
  - 20) Maheswari B K, Truman K Z , Gould P L and Naggar El (2005), “Three dimensional nonlinear seismic analysis of single piles using FEM model :effects of plasticity of soil”, *International journal of Geomechanics*, Vol. 5, pp 35-44.
  - 21) Hui xiong, Xilin L and Liang H (2005) , “Simplified dynamic finite-element analysis for three-dimensional pile-grouped-raft-high-rise buildings”, *Sixth International Conference on Tall Buildings, Mini Symposium on Sustainable Cities, Mini Symposium on Planning, Design and Socio-Economic Aspects of Tall Residential Living Environment*.

# Appendix 1

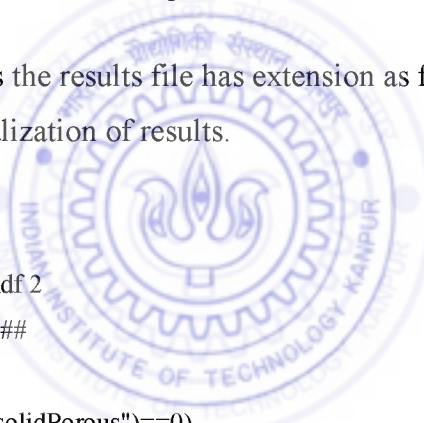
---

## Interface between Opensees and Gid

As Opensees does not have an Graphic user interface, Gid is used as a pre and post processor. Problem type can be created for generation of input file for opensees. The details of the Interface is given below. This Interface contains 5 files.

1. .bas file
2. .mat file which specifies the details of materials
3. .cnd file which specifies boundary conditions of the problem
4. .prb file which contains problem data
5. .tcl file, an interface between opensees and Gid

After solving the analysis the results file has extension as filename.flavia.res. This file is readable by Gid for visualization of results.



```
wipe all
model BasicBuilder -ndm 2 -ndf 2
#####Define materials#####
*loop materials
*if(strcmp(MatProp(1),"FluidsolidPorous")==0)
*set var E(real)=Operation(MatProp(youngs_modulus(KN/cu.m),real))
*set var pois(real)=Operation(MatProp(poissons_ratio,real))
*set var G(real)=operation(E/(2*(1+pois)))
*set var B(real)=operation(E/(3*(1-2*pois)))
*set var Bdf(real)=Operation(1*MatProp(MassDensity(t/cu.m),real))
nDMaterial PressureDependMultiYield *Operation(matnum()+1) 2 *MatProp(2) *G *B *MatProp(6)
*MatProp(7) *MatProp(8) *MatProp(9) *MatProp(10) *MatProp(11) *MatProp(12) *MatProp(13) 0 0 0
nDMaterial FluidSolidPorous *matnum() 2 2 *B
*elseif(strcmp(MatProp(1),"Concrete")==0)
nDMaterial ElasticIsotropic *Operation(matnum()+1) *MatProp(3) *MatProp(4)
*set var Bdf1(real)=Operation(1*MatProp(MassDensity(t/cu.m),real))
*end if
*end materials
```

```

updateMaterialStage -material 1 -stage 0
updateMaterialStage -material 2 -stage 0
#####Define nodes#####
*loop nodes
node *NodesNum *Nodescoord(1,real) *Nodescoord(2,real)
*end nodes
#####Define elements#####
*Set elems(All)
*Remove elems(Linear)
*loop elems
*if(Operation(ElemsMat+1)==2)
element quad *ElemsNum *ElemsConec 1.0 "PlaneStrain" *Operation(ElemsMat+1) *Bdf 0 0 0
*elseif(Operation(ElemsMat+1)==3)
element quad *ElemsNum *ElemsConec 1.0 "PlaneStrain" *Operation(ElemsMat+1) *Bdf1 0 0 0
*endif
*Set var num(int)=Elemsnum
*end elems
*Set var addMat(int)=0
#####
*loop materials
*if(strcmp(MatProp(1),"Plane")==0)
*Set elems(All)
*Remove elems(Linear)
*loop elems
*end elems
*elseif(strcmp(MatProp(1),"ZeroLength")==0)
*Set var addMat(int)=Operation(addMat+1)
*Add elems(Linear)
*Remove elems(Quadrilateral)
uniaxialMaterial Elastic *Operation(matnum()+1) *MatProp(2) *MatProp(4)
uniaxialMaterial Elastic *operation(addMat+nmats+1) *MatProp(3) *MatProp(5)
*loop elems
*if((matnum == ElemsMat)|(operation(addMat+nmats)== ElemsMat))
element zeroLength *ElemsNum *ElemsConec -mat *Operation(ElemsMat+1)
*Operation(addMat+nmats+1) -dir 1 2
*endif
*end elems

```

```

*endif
*end materials
region 1 -eleRange 1 *num -rayleigh *Gendata(11) *Gendata(12) 0 0
*loop materials
*elseif(strcmp(MatProp(1),"ZeroLength")==0)
*Set var addMat(int)=Operation(addMat+1)
*Add elems(Linear)
*Remove elems(Quadrilateral)
*loop elems
*if((matnum == ElemsMat)||(operation(addMat+nmats)== ElemsMat))
*endif
*end elems
*end materials
*set cond Point-Constraints *nodkahes
*loop nodes *onlyincond
fix *nodesnum *cond(1) *cond(2)
*end
*set cond staticload *nodkahes
*loop nodes *onlyincond
pattern Plain 3 Linear {
    load *nodesnum *cond(1) *cond(2);
}
*end

*# find the equalDOF nodes
*set Cond Point-Master-Slave *nodes *CanRepeat
*loop nodes *OnlyInCond
*if(strcmp(cond(1),"Master")==0)
*set var mx(real)=NodesCoord(1)
*set var my(real)=NodesCoord(2)
equalDOF *NodesNum *\ 
*loop nodes *OnlyInCond
*if((strcmp(cond(1),"Slave")==0)&&(NodesCoord(1)==mx)&&(NodesCoord(2)==my))
*NodesNum 1 2
*endif
*end nodes
*endif

```

```

*end nodes

*set cond mass *nodkahes
*loop nodes *onlyincond
mass *nodesnum *cond(1) *cond(2)
*end

#####Apply gravity#####
system ProfileSPD
test NormDispIncr 1.e-12 25 0
constraints Transformation
integrator LoadControl 1 1 1
algorithm Newton
numberer RCM
# create the Analysis
analysis Static
#analyze
analyze 2
puts "gravity load applied"
puts "Pressure dependent mulyield material"
puts "Seismic excitation applied"
puts "Transient Analysis in progress"
puts "WAIT"
setTime 0.0
wipeAnalysis

#####Apply displacement time history#####
set DispSeries "Series -dt 0.005 -filePath motion.G3 -factor 1";
*set cond seismic_load *nodkahes
pattern MultipleSupport 1 {
groundMotion 2 Plain -disp $DispSeries
*set cond seismic_load *nodes
*loop nodes *onlyincond
imposedMotion *nodesnum *cond(1) 2
*end
}
#####Transient analysis parameters#####

```

```

constraints Penalty 1.0e18 1.0e18 ;# Transformation; #
test NormDispIncr 1.e-12 25 0
algorithm Newton
numberer RCM
system ProfileSPD
integrator Newmark 0.5 0.25
analysis Transient
#####Recorders for displacement and acceleration#####
recorder Node -file *Gendata(13).flavia.res -time -node all -dof 1 2 -dT *Gendata(2) disp
recorder Node -file *Gendata(14).flavia.res -time -node all -dof 1 2 -dT *Gendata(2) accel
set startT [clock seconds]
analyze *Gendata(3) *Gendata(2)
set endT [clock seconds]
puts "Execution time: [expr $endT-$startT] seconds."
puts "Transient analysis done"

```

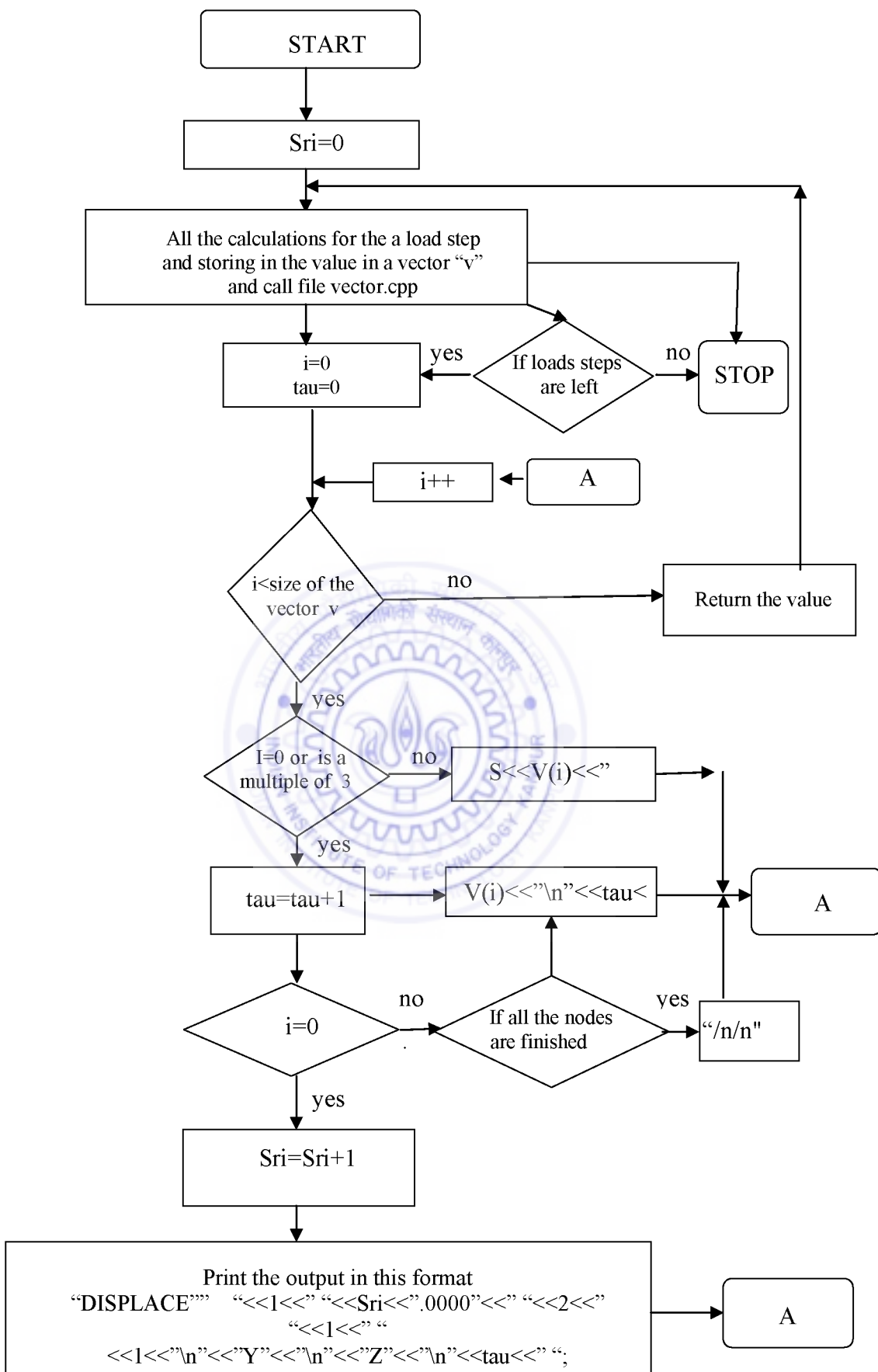


## Appendix 2

---

OpenSees is a program written in C++ having different classes and objects. The final output in the OpenSees program is handled by the DataOutputHandler.cpp, which calls vector.cpp, which transfers the value in the required file. After each iteration the total number of values calculated are stored in a vector. The values stored in the vector are the time steps and the displacement of the nodes in the order X, Y. The source code was edited in vector.cpp file so that the required form of output is obtained. The flow chart shows the steps of editing. The new Opensees.exe file creates results in a format readable by Gid and this is useful for 2-d analysis to visualize the results in the form of contours. Two new variables are added in the file vector.cpp, “sri” and “tau”. Variable “Sri” calculates the time step and tau keeps the note of the node number. The program was edited from line number 1064 of vector.cpp. Below the actual interface is given.

```
float tau;
double sri=0.0025;
//friend OPS_Stream &operator<<(OPS_Stream &s, const Vector &V)
//A function is defined to allow user to print the vectors using OPS_Streams.
OPS_Stream &operator<<(OPS_Stream &s, const Vector &V)
{
for (int i=0,tau=0; i<V.Size(); i++)
{
    if ( i==0 || i%2 == 0 )
    {
        tau++;
        if (i==0) {
            sri+=0.0025;
            // Header for Gid results
            s<<"DISPLACE"<<" "<<" "<<" "<<1<<" "<<sri<<" "<<2<<" "<<1<<
            <<1<<"\n"<<"X"<<"\n"<<"Y"<<"\n"<<tau<<" ";
        }
        else {
            if (tau == ((V.Size()-1)/2)+1)
                s <<V(i)<<"\n\n";
            else s <<V(i)<<"\n"<<tau<<" ";
        }
    }
    else s << V(i) << " ";
}
return s << endl;
}
```



## APPENDIX 3 : INPUT EARTHQUAKE MOTION

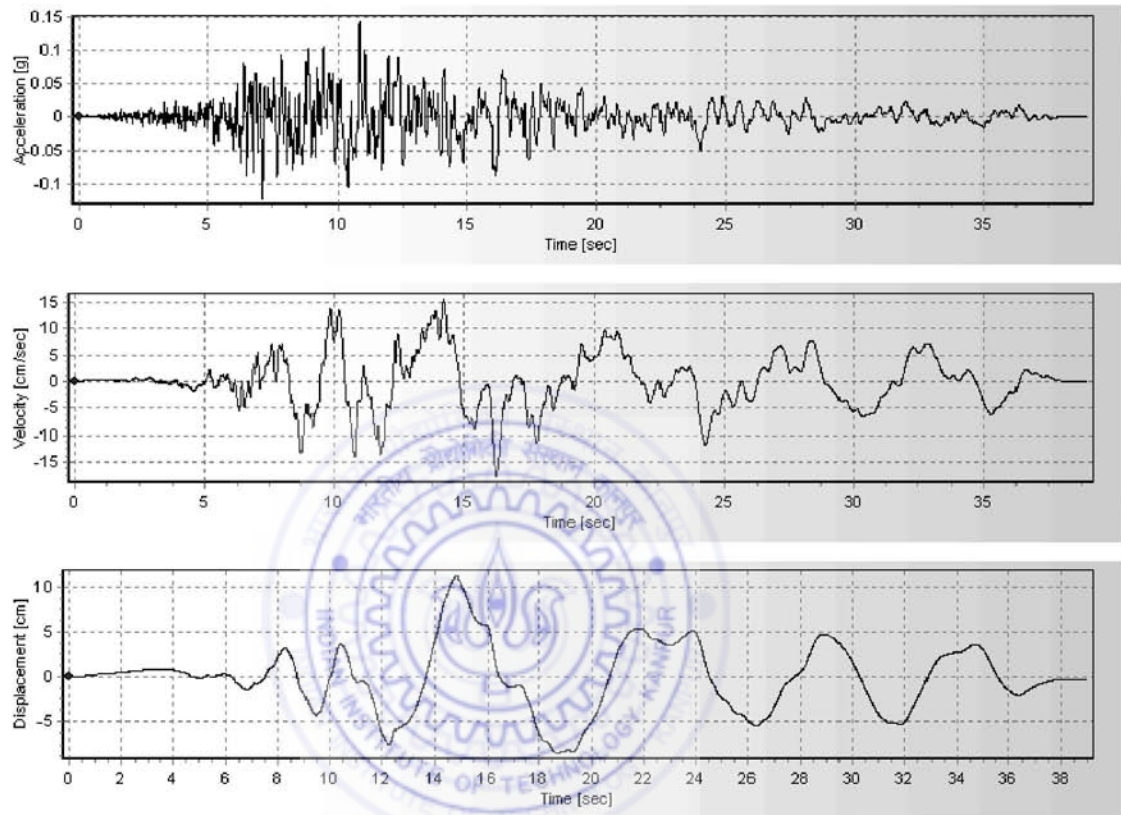


**Figure A3.1:** Acceleration, velocity and displacement time history of the input

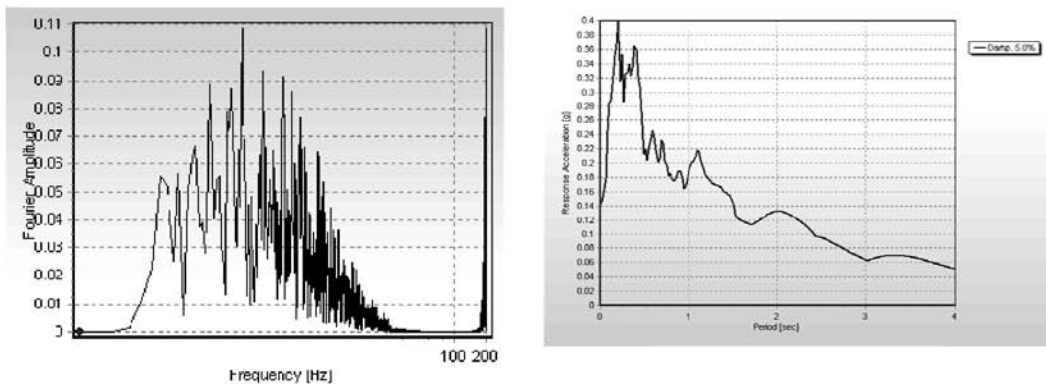


**Figure A3.2:** Fourier spectrum of the input motion and Response spectrum (5 % damping)

## **Ground motion parameters**

Maximum Acceleration: 0.1433283g at time t=10.845sec

Maximum Velocity: 17.58683057cm/sec at time t=16.2sec

Maximum Displacement: 11.18472242cm at time t=14.835sec

$V_{max} / A_{max}$ : 122.70312682sec

Acceleration RMS: 0.02518754g

Velocity RMS: 4.96506028cm/sec

Displacement RMS: 3.74857679cm

Arias Intensity: 0.38131222m/sec

Characteristic Intensity (Ic): 0.02496542

Specific Energy Density: 961.54437889cm<sup>2</sup>/sec

Cumulative Absolute Velocity (CAV): 0.63997383cm/sec

Acceleration Spectrum Intensity (ASI): 0.12851759g\*sec

Velocity Spectrum Intensity (VSI): 73.64537078cm

Sustained Maximum Acceleration (SMA): 0.1048294g

Sustained Maximum Velocity (SMV): 13.87196592cm/sec

Effective Design Acceleration (EDA): 0.13311107g

A95 parameter: 0.14006629g

Predominant Period ( $T_p$ ): 0.2sec

Mean Period ( $T_m$ ): 0.62864478sec

Predomonant frequency of excitation : 3.125 Hz

# Appendix 4

## DISPLACEMENT RESPONSE



Figure A4.1 : Free-field response of the model

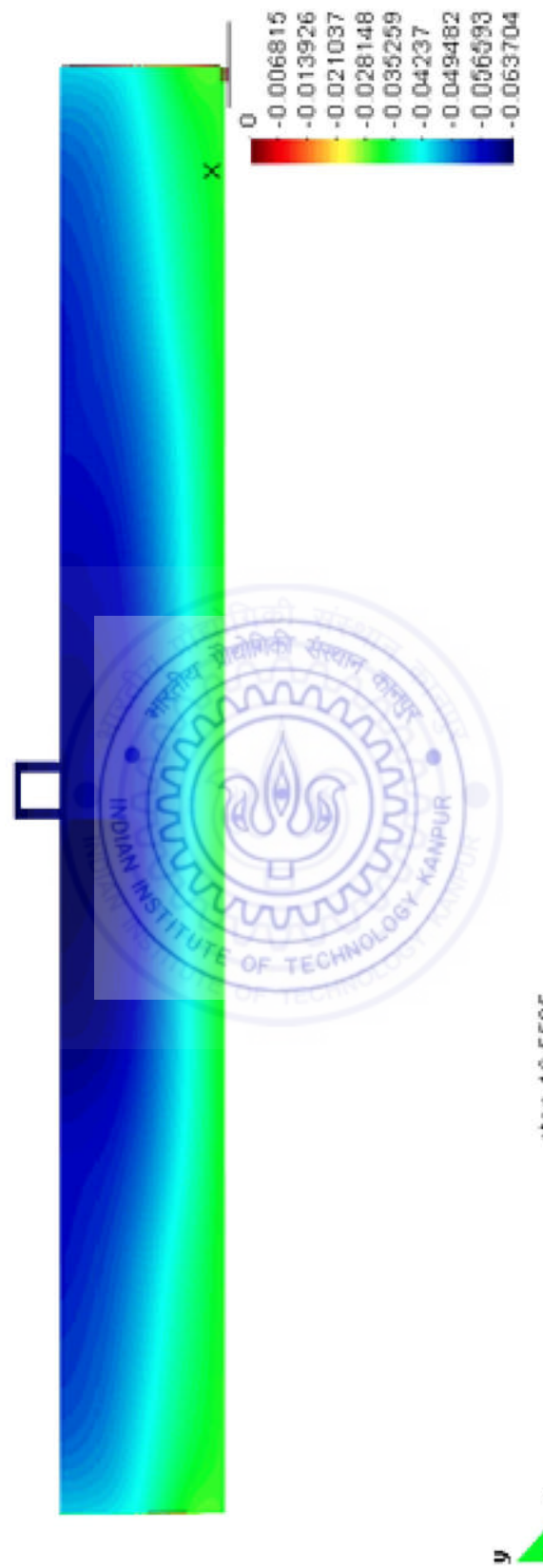
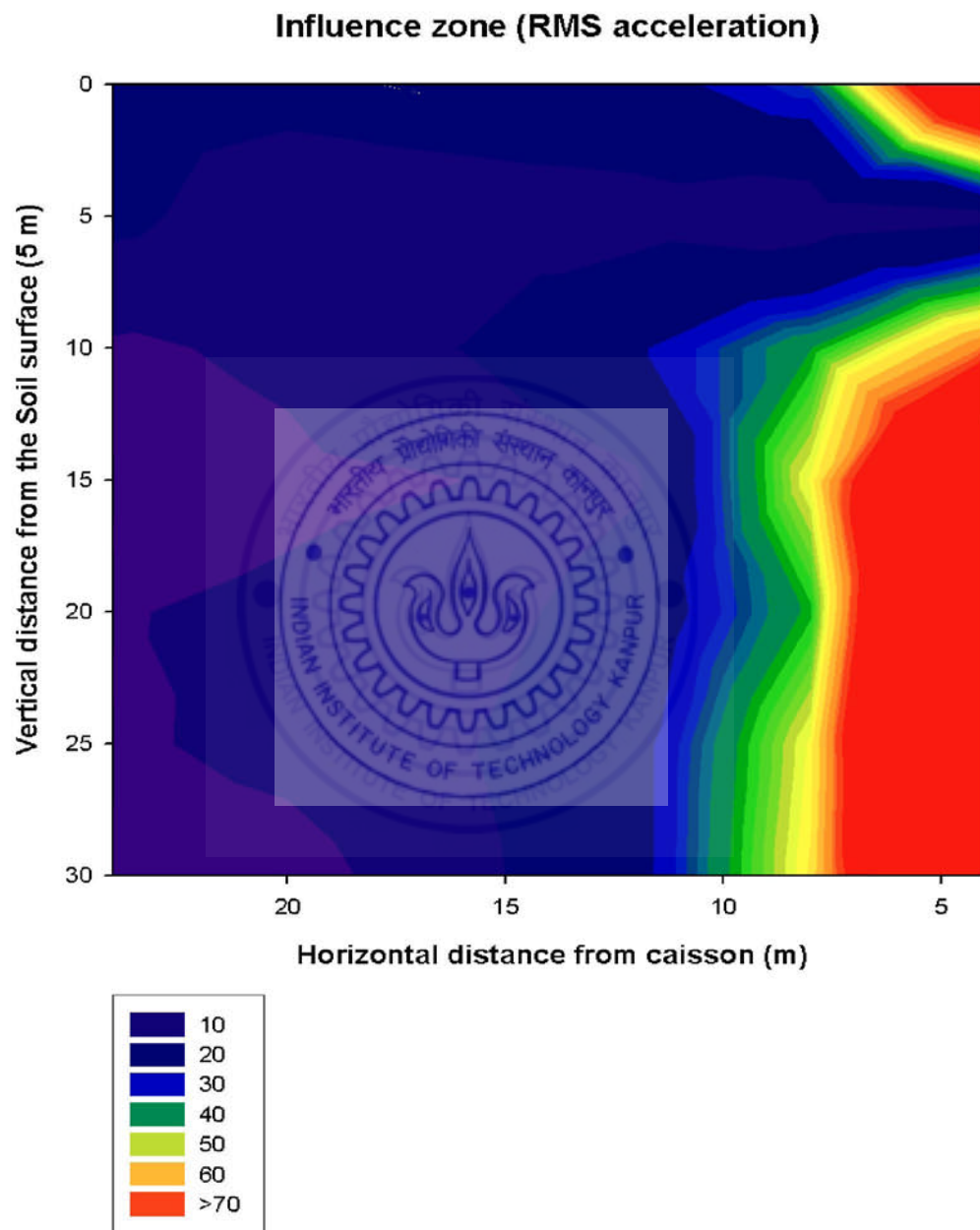


Figure A4.2 : Displacement response of soil caisson model

# Appendix 5

## INFLUENCE ZONE CONTOUR



**Figure A 5.1 Variation of RMS acceleration with depth for soil-caisson with interface elements with less contour interval**

## Appendix 6

### RESPONSE SPECTRUM AT A DISTANCE OF 20M FROM CAISSON INTERFACE (WITH CONTACT ELEMENTS)

